MIT
International Center for
Air Transportation

COMPARISON OF METHODS FOR EVALUATING IMPACTS OF AVIATION NOISE ON COMMUNITIES

Morrisa A. Brenner and R. John Hansman

This report is based on the Masters Thesis of Morrisa A. Brenner submitted to the Department of Aeronautics and Astronautics in partial fulfillment of the requirements for the degree of Master of Science at the Massachusetts Institute of Technology.

The work presented in this report was also conducted in collaboration with:

Prof. R. John Hansman

Report No. ICAT-2017-05
May 2017

MIT International Center for Air Transportation (ICAT)
Department of Aeronautics & Astronautics
Massachusetts Institute of Technology
Cambridge, MA 02139 USA

Technical Report Documentation Page

1. Report No.	2. Government Accession No.	3. Recipient's Catalog No.
ICAT-2017-05		

4. Title and Subtitle	5. Report Date
Comparison of Methods for Evaluating Impacts of Aviation Noise on Communities	July 2017
	6. Performing Organization Code

7. Author(s)	8. Performing Organization Report No.
Brenner, Morrisa A., R. John Hansman	

9. Performing Organization Name and Address	10. Work Unit No. (TRAIS)
Center of Excellence for: Alternative Jet Fuels and Environment Massachusetts Institute of Technology Department of Aeronautics & Astronautics Cambridge, MA 02139	11. Contract or Grant No. 13-C-AJFE-MIT-008

12. Sponsoring Agency Name and Address	13. Type of Report and Period Covered
Federal Aviation Administration Office of Environment and Energy	Technical Report
	14. Sponsoring Agency Code

15. Supplementary Notes

http://hdl.handle.net/1721.1/110791

16. Abstract

Community opposition to the noise concentration from precise NextGen Performance-Based Navigation (PBN) aircraft arrival and departure procedures poses a significant threat to the future of these procedures in the U.S. National Airspace System. A substantial number of complaints concerning airport noise come from locations outside the 65dB Day-Night Level (DNL) contour considered the significant noise exposure threshold in U.S. federal regulation. This indicates that this threshold does not sufficiently capture areas that experience annoyance related to more concentrated, lower level overflight noise at distances farther from the airport. This thesis assesses the effectiveness by which different noise analysis methods capture the locations of these airport noise complaints through examination of the noise exposure for three representative scenarios at Boston Logan International Airport using DNL and number of overflights above a noise threshold (Nabove) metrics. The three scenarios examined include the standard noise analysis methodology scenario (annual average day) as well as a day of heavy usage of a noise-sensitive runway (33L for departures), and a scenario representing a peak hour of departures on this runway. The results indicate that the 33L peak day scenario does a better job of capturing a substantial fraction of the complainants sensitive to the 33L departure trajectories (66%-87% at the 45dB-50dB DNL thresholds) than the standard annual average day scenario. Results for the 33L peak day scenario indicate that the Nabove metric is also effective at capturing noise complaints at the 60dB day/50dB night noise threshold at exposure rates in the 25-50 overflight range (78%-84% complainant capture).

17. Key Words	18. Distribution Statement
air transportation, aviation noise, aircraft noise, Day-Night Level (DNL), ASCENT	

19. Security Classif. (of this report)	20. Security Classif. (of this page)	21. No. of Pages	22. Price
Unclassified	Unclassified		

Page Intentionally Left Blank

COMPARISON OF METHODS FOR EVALUATING IMPACTS OF AVIATION NOISE ON COMMUNITIES

by

Morrisa A. Brenner and Prof. R. John Hansman

ABSTRACT

Community opposition to the noise concentration from precise NextGen Performance-Based Navigation (PBN) aircraft arrival and departure procedures poses a significant threat to the future of these procedures in the U.S. National Airspace System. A substantial number of complaints concerning airport noise come from locations outside the 65dB Day-Night Level (DNL) contour considered the significant noise exposure threshold in U.S. federal regulation. This indicates that this threshold does not sufficiently capture areas that experience annoyance related to more concentrated, lower level overflight noise at distances farther from the airport. This thesis assesses the effectiveness by which different noise analysis methods capture the locations of these airport noise complaints through examination of the noise exposure for three representative scenarios at Boston Logan International Airport using DNL and number of overflights above a noise threshold (N_{above}) metrics. The three scenarios examined include the standard noise analysis methodology scenario (annual average day) as well as a day of heavy usage of a noise-sensitive runway (33L for departures), and a scenario representing a peak hour of departures on this runway. The results indicate that the 33L peak day scenario does a better job of capturing a substantial fraction of the complainants sensitive to the 33L departure trajectories (66%-87% at the 45dB-50dB DNL thresholds) than the standard annual average day scenario. Results for the 33L peak day scenario indicate that the N_{above} metric is also effective at capturing noise complaints at the 60dB day/50dB night noise threshold at exposure rates in the 25-50 overflight range (78%-84% complainant capture).

Page Intentionally Left Blank

ACKNOWLEDGEMENTS

The author would like to thank Massport for access to the complaint data that made the analysis in this thesis possible. The author would also like to thank Luke Jensen, Jacqueline Thomas, and Cal Brooks, who contributed to work used or referenced in this report.

This work was sponsored by the Federal Aviation Administration (FAA) under ASCENT Center of Excellence Project 23, Cooperative Agreement 13-C-AJFE-MIT-008. Opinions, interpretations, conclusions, and recommendations are those of the authors and are not necessarily endorsed by the United States Government.

Page Intentionally Left Blank

Table of Contents

List of Figures

List of Tables

Page Intentionally Left Blank

List of Equations

Page Intentionally Left Blank

Chapter 1 Introduction

1.1 Motivation

The rollout of Performance-Based Navigation (PBN) procedures as part of the FAA's NextGen program paves the way for improvements in safety and efficiency within the U.S. National Airspace [1]. As PBN-based arrival and departure procedures have been implemented at airports around the country, however, changes in noise patterns for the areas surrounding these airports have led to increases in community opposition to the use of these new procedures. In some places, new procedures have been rolled back due to this organized community opposition to aviation procedural changes.

One area of particularly strong interest and a focus of community activism against implementation of PBN procedures at airports across the nation relates to changes in the dispersion of aircraft flying published procedures – as PBN procedures are implemented the degree of accuracy to which aircraft follow required lateral paths increases substantially. This leads to a concentration of aircraft lateral trajectories flying PBN procedures compared to those flying non-PBN procedures, an effect that can be seen in Figure 1.

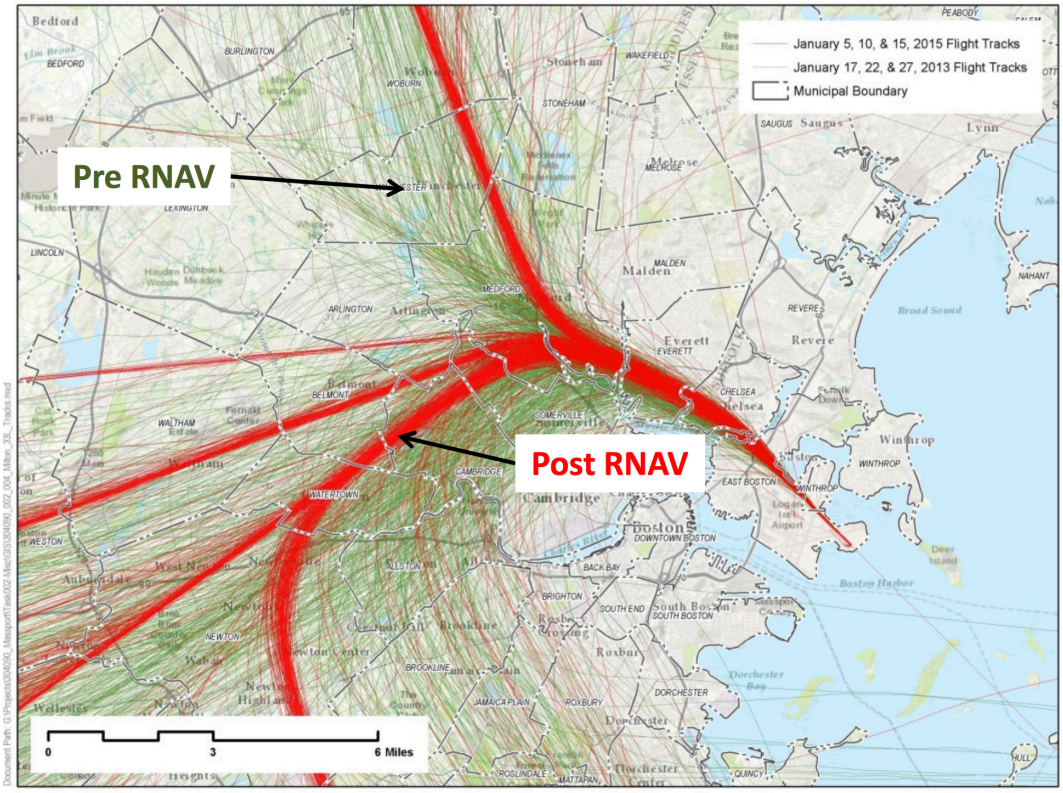

Figure 1: Changes in Flight Track Dispersion Due to Implementation of RNAV PBN Procedure for Runway 33L Departures at BOS. Source: Massport [2]

While analysis of noise impacts is required as part of the process for approval for new approach or departure procedures, the level of community opposition to the rollout of these procedures despite this analysis indicates that limitations exist in this analysis process. This can be seen in Figure 2. In this figure, the base map shows the location of noise complainants between August 2015 and July 2016 at Boston Logan International Airport (BOS) on top of ASDE-X departure flight tracks for 12 days in 2015-16. The overlay shows the official noise exposure contours for BOS in 2015, with the purple contour corresponding to the 65dB DNL level of noise considered significant according to U.S. federal regulation. The fact that such a substantial fraction of complainants occur outside this 65dB DNL contour considered the significant aviation noise exposure level underscores the need for more careful examination of the methods used to evaluate noise impact. The left-hand map of Figure 3 shows the same complainant locations and flight tracks as Figure 2, and the right-hand map of Figure 3 shows the same complainant locations on top of ASDE-X arrival flight tracks from the same 12 days in 2015-16.

These maps show that the locations of complaints tend to be tied to particular streams of departure or arrival flights, as most of the clusters of complaint locations are near either a large number of departure flight tracks or near a large number of arrival flight tracks.

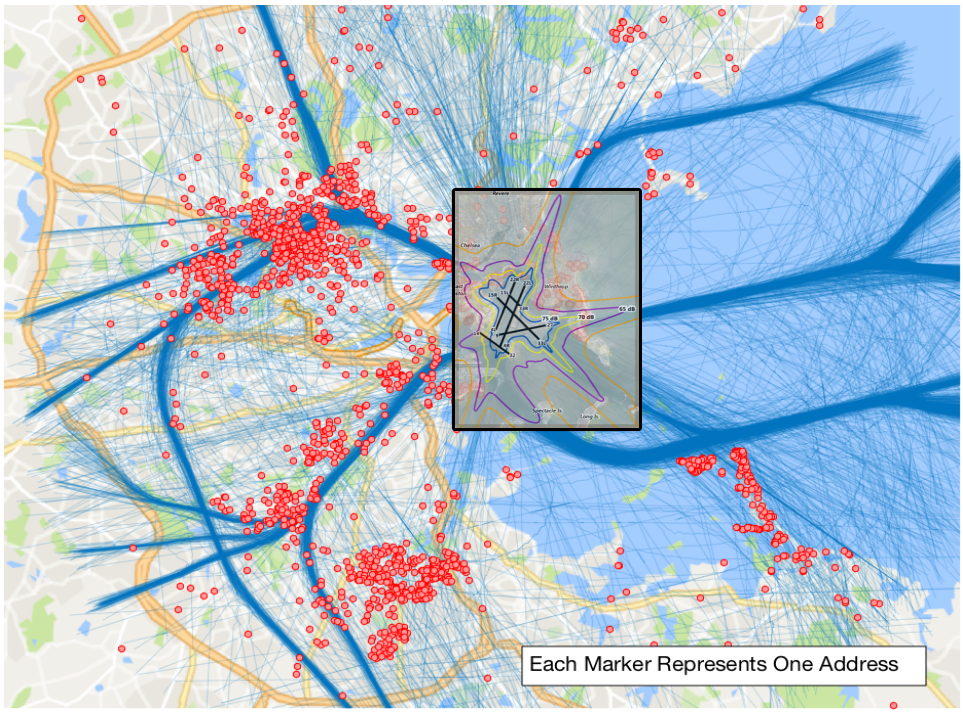

Figure 2: 2015 Departure Flight Tracks at BOS, with Complaint Locations and Official Annual Average DNL Contours; Regulatory Significant Exposure Contour of 65dB DNL is Purple. Overlay Source: Massport [3]. Complainant Map Source: Hansman [2]

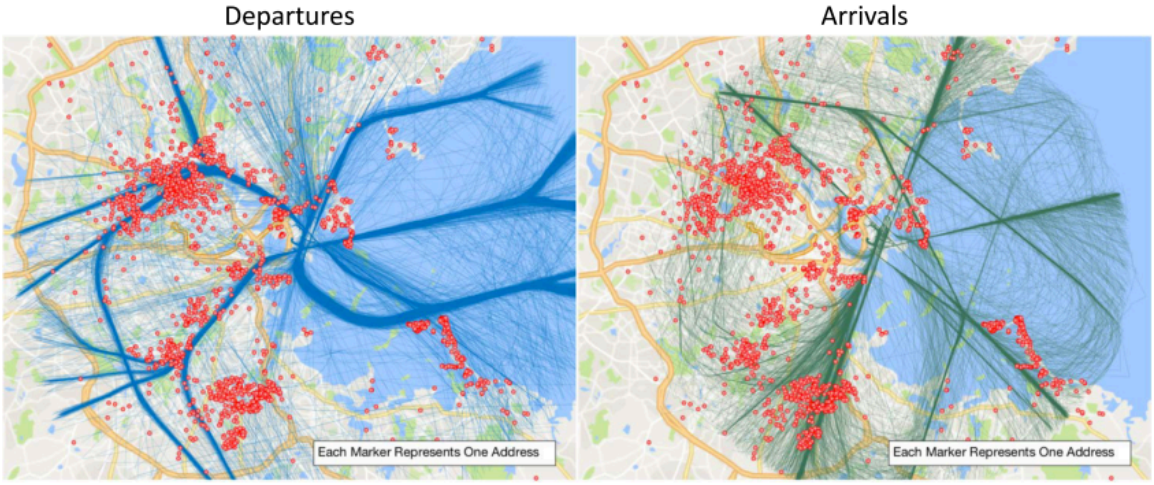

Figure 3: 2015 Arrival (left) and Departure (right) Flight Tracks at BOS, with Complaint Locations in Red. Source: Hansman [2]

1.2 Research Objective and Scope

This research seeks to examine a series of noise impact analysis methods in the context of community resident reactions to noise and to examine their effectiveness in identifying hotspots of annoyance. A series of representative scenarios at Boston Logan International Airport (BOS) based on actual flight tracks and schedule data will be modeled using a combination of tools developed at MIT and industry-standard noise analysis methods. Three scenarios will be examined: an annual average day, a representative day of heavy usage of a single runway for departures (runway 33L), and a day reflecting the peak hour of departure operations on this 33L peak day. Scenarios representative of actual daily usage of particular runways are examined in addition to the annual average day typically utilized for noise impacts analysis since complaint locations are often associated with utilization of specific runways for departures or arrivals. Noise impact results will then be compared to the locations of complaints regarding noise at BOS using a series of noise metrics, and results will be evaluated based on the degree to which the quantified noise exposure captures these complaint locations. The complaint data used is from a 12-month period similar to that from which the flight tracks and scenario schedules are drawn. Complaint locations are used as they represent the best available data for measuring annoyance and also likely capture the level of activism and opposition of citizens in different areas. If a goal is to understand or predict the level of community activism that prevents PBN-enabled benefits from being rolled out at an airport, complaint locations are likely to be a useful basis for the evaluation of noise impacts.[1]

Annual average noise exposure results will also be compared to official annual average noise exposure results to provide context for the modeled results. Observations will then be made regarding the degree to which each of these representative scenarios captures complaint locations, and regarding the degree to which noise exposure captures complaint locations when measured using two different metrics.

---

[1] It is important to note that while complaint patterns likely identify hotspots of perceived noise impact, complaints, by their nature, are self-disclosed and individual complaints may not directly reflect general adverse noise impact.

Chapter 2 Background

2.1 Sound and Loudness

Humans perceive fluctuations in atmospheric pressure as sound, and noise is unwanted sound [4]. The perceived loudness of a sound is related to the amplitude of these fluctuations as well as the frequency [4]. There is a specific range of frequencies audible to humans, and this narrows somewhat with age [4]. Since humans are annoyed to different extents by sound from similar amplitudes of different frequency fluctuations, various frequency-weighting scales have been developed to capture the annoyance experienced by humans as a response to different spectral compositions of sound [4]. These, along with the metrics used to capture the sound "experience" of an event, will be discussed further in the following sections. The relative sound levels of a variety of specific noise sources using a common frequency-weighting scheme are shown in Figure 4.

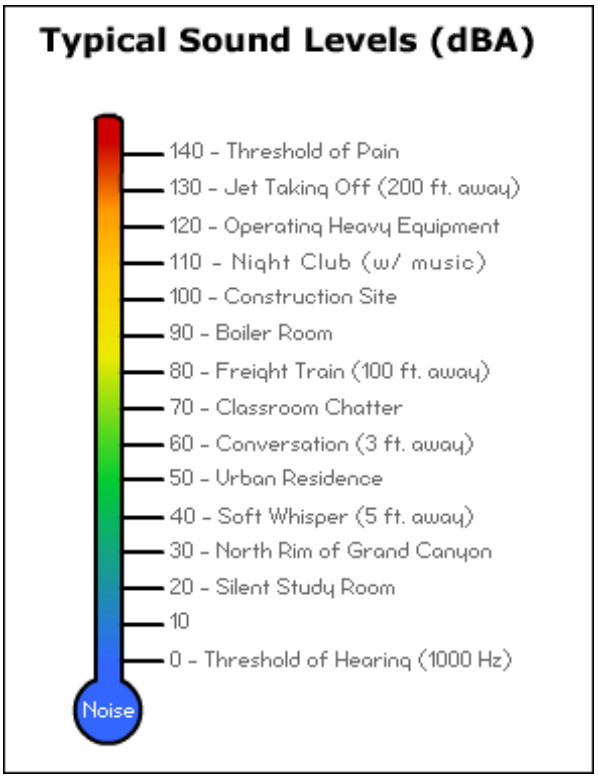

Figure 4: Common Sounds on an Instantaneous A-Weighted dB Scale. Source: OSHA [5]

2.2 Introduction to Aviation Noise Analysis

As explained in Section 2.1, the loudness of a noise depends on the frequency and amplitude composition of a sound. To allow for comparison of noise between sounds with different frequency compositions, different frequency-weighting schemes have been developed. Three of these are sufficiently well recognized in the context of aviation noise analysis to have been included in common aviation noise analysis tools. These three types of sound spectral weighting are A-weighting, C-weighting, and tone-corrected perceived noise [6]. A-weighting is designed to reflect people's perceptions of the loudness of events, C-weighting is designed to do something similar but focuses on distinctions among already loud events (above 90 decibels (dB)), and tone-corrected perceived noise aims to capture the loudness of events with aircraft-like spectral compositions [6]. A-weighted metrics are the most commonly used, however, and as will be discussed in Section 2.3, they are the basis for much of the noise-related aviation regulation in the United States. For this reason, metrics based on an A-weighted frequency spectrum will be the only ones discussed in this thesis.

Aviation noise metrics fall into a few categories, two of which will be explored in this thesis: exposure-based metrics and maximum sound level metrics [6]. Exposure-based metrics aim to capture a combination of the duration and peaks of noise events, while maximum sound level metrics focus on the magnitude of the peaks of events. Most quantitative impact results derived from these metrics are expressed on the logarithmic decibel (dB) scale, where an increase of roughly 3dB corresponds to a doubling in the intensity of a sound [4].

The noise impact of aviation activity around an airport is ultimately driven by the noise impact of each discrete aviation event. Section 2.2.1 will provide an overview of some commonly used metrics for measuring the impact of individual flight operations (single event noise metrics) and Section 2.2.2 will introduce multiple event impact metrics derived from these single event impact metrics.

2.2.1 Single Event Aviation Noise Metrics

2.2.1.1 Maximum Sound Level Metric: $L_{A,max}$

The A-weighted maximum sound level noise metric is known as $L_{A,max}$ (or LAMAX) and is simply the maximum instantaneous A-weighted sound level at a given observer location [6]. A mathematical representation for $L_{A,max}$ at an observer location is given in Equation 1, where L(t) is the sound pressure level over time and T is the end of the aviation overflight of interest.

Equation 1: Formula for $L_{A,max}$. Source: HMMH [7]

$$L_{A,max} = \max\big(L(t)\big), t \in [0, T]$$

2.2.1.2 Exposure-Based Metric: SEL

The A-weighted single event exposure-based noise metric is called Sound Exposure Level, or SEL [6]. The goal of SEL is to quantify the overall noisiness of an overflight by combining both the duration and peak sound levels of the event. This is accomplished by integrating the portions of the sound pressure level (SPL) time trace of an aviation overflight within 10dB of $L_{A,max}$[2] and normalizing the integral by a fixed time period (usually one second) [8] [7]. A graphical depiction of SEL computation is shown in Figure 5 from Trani [8], where the orange shaded region represents the region that is integrated to generate SEL. The formula used to calculate SEL follows in Equation 2, where L(t) is the SPL over time, t_1 and t_2 bound the region where sound is within 10dB of the peak, and t_0 is the reference time over which the integral is normalized.[3]

---

[2] This implies that for SEL to be defined for an overflight, $L_{A,max}$ must be at least 10dB higher than whatever SPL is considered the floor. If this were not the case, SEL would be infinite.

[3] As will be discussed in Section 2.3.2, however, the standard method used for calculation of SEL in aviation industry noise analysis is not directly from a time history of sound pressure level.

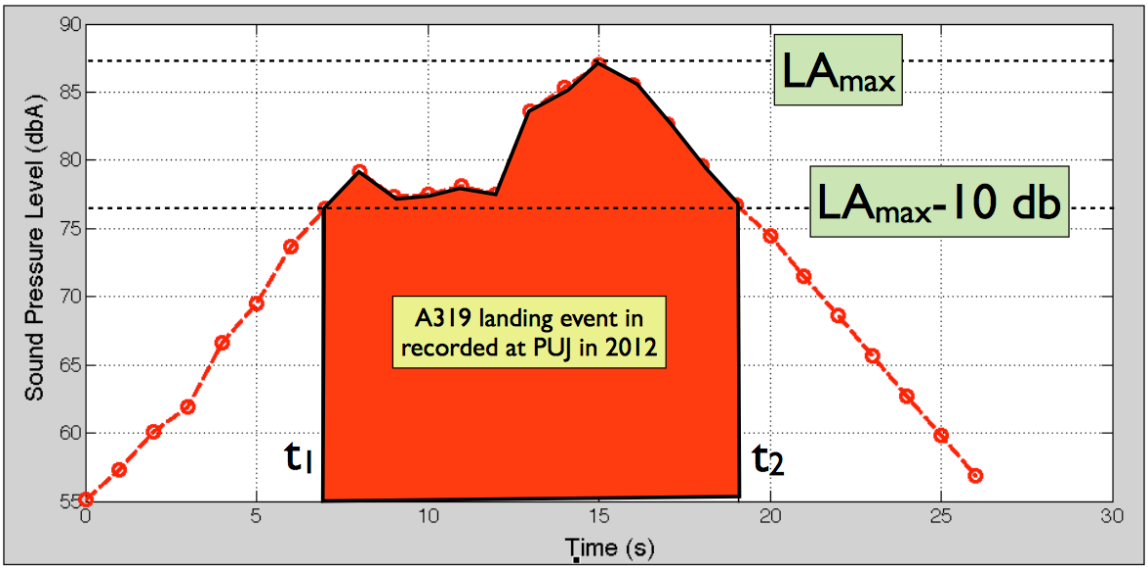

Figure 5: SEL Calculation for a Single Flyover Event. Source: Trani [8]

Equation 2: Formula for SEL. Source: Trani [8]

$$SEL = 10 * log_{10}\left(\frac{1}{t_0}\int_{t_1}^{t_2} 10^{\frac{L(t)}{10}} dt\right)$$

2.2.2 Multiple Event Aviation Noise Metrics

2.2.2.1 Maximum Sound Level Metric: N_{above}

A maximum sound level noise metric often used in aviation noise analysis is the number of flights above a threshold $L_{A,max}$, called N_{above}. Since N_{above} essentially just counts the number of individual events with noise above a selected threshold at a given observer location, it is very simple to compute and to understand. A mathematical representation for N_{above} at a given observer location is given in Equation 3. N_{above} is commonly calculated on the basis of total overflights during a 24-hour period.

Equation 3: Formula for N_{above}

$$N_{above} = \sum_{i=1}^{n_{day}} x_{i,day} + \sum_{i=1}^{n_{night}} x_{i,night}$$

$$x_{i,day} = 1 \; if \; L_{A,max} > threshold_{day}, x_{i,day} = 0 \; otherwise$$

$$x_{i,night} = 1 \; if \; L_{A,max} > threshold_{night}, x_{i,night} = 0 \; otherwise$$

It is often useful to think about N_{above} in terms of the average time between overflights during the interval of interest. The relationship between the average time between overflights and daily N_{above} is shown in Figure 6.

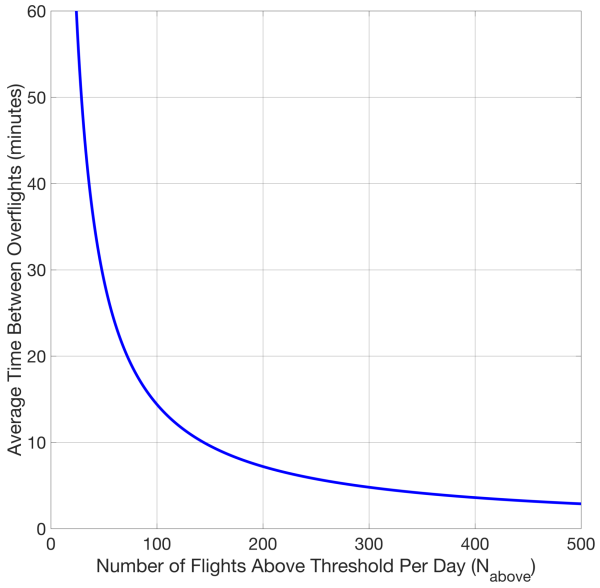

Figure 6: Relationship Between Average Time Between Overflights and Daily N_{above}

2.2.2.2 Exposure-Based Metric: DNL

The multiple event exposure-based metric most commonly used in aviation noise analysis is called the Day-Night Level (DNL). DNL is a logarithmic summation of noise exposure from individual noise events quantified using SEL. DNL takes the SEL values for a series of individual events at an observer location and logarithmically adds and averages these values over a 24-hour period, applying a noise penalty to night operations (which are defined as those occurring between 10pm and 7am local time) [6] [7]. This 10dB penalty is captured by applying by a weighting factor of 10dB to the SEL for each nighttime operation [6] [7]. Computation of DNL from SEL is shown in Equation 4, where the time constant T refers to the overall analysis time scale. For typical analysis using DNL, T = 24 hours = 86,400 seconds.

Equation 4: Formula for DNL. Source: HMMH [7]

$$DNL = 10 * log_{10}\left(\frac{1}{T}\left[\sum_{i=1}^{n_{day}} 10^{\frac{SEL_{i,day}}{10}} + \sum_{i=1}^{n_{night}} 10^{\frac{SEL_{i,night}+10}{10}}\right]\right)$$

In practice, the analysis period T is often removed from the inside of the logarithm and added to the un-weighted logarithmically added SEL. This equation, which is mathematically equivalent to Equation 4, is shown in Equation 5.

Equation 5: Formula for DNL with Separated Time Constant. Source: HMMH [7]

$$DNL = 10 * log_{10}\left(\left[\sum_{i=1}^{n_{day}} 10^{\frac{SEL_{i,day}}{10}} + \sum_{i=1}^{n_{night}} 10^{\frac{SEL_{i,night}+10}{10}}\right]\right) - 10 * log_{10}(T)^{4}$$

As a result of the logarithmic addition of SEL that forms the basis for DNL, the contribution to DNL of an additional overflight decreases with the total number of overflights. This can be seen in Figure 7, where each curve shows the DNL from a given number of operations at the same SEL. This shows that as the number of operations with equivalent SEL increases, each additional operation increases DNL by a smaller and smaller amount.

[4] AEDT, which will be introduced later in Section 2.3.2, uses a rounded value for the separated time constant of 49.37 [6]. The toolset used for analysis in this thesis, however, does not round the time constant and uses $10 * log_{10}(86{,}400)$ in each calculation. This has been seen to lead to a small difference in DNL values computed using the thesis analysis toolset and those calculated directly in AEDT.

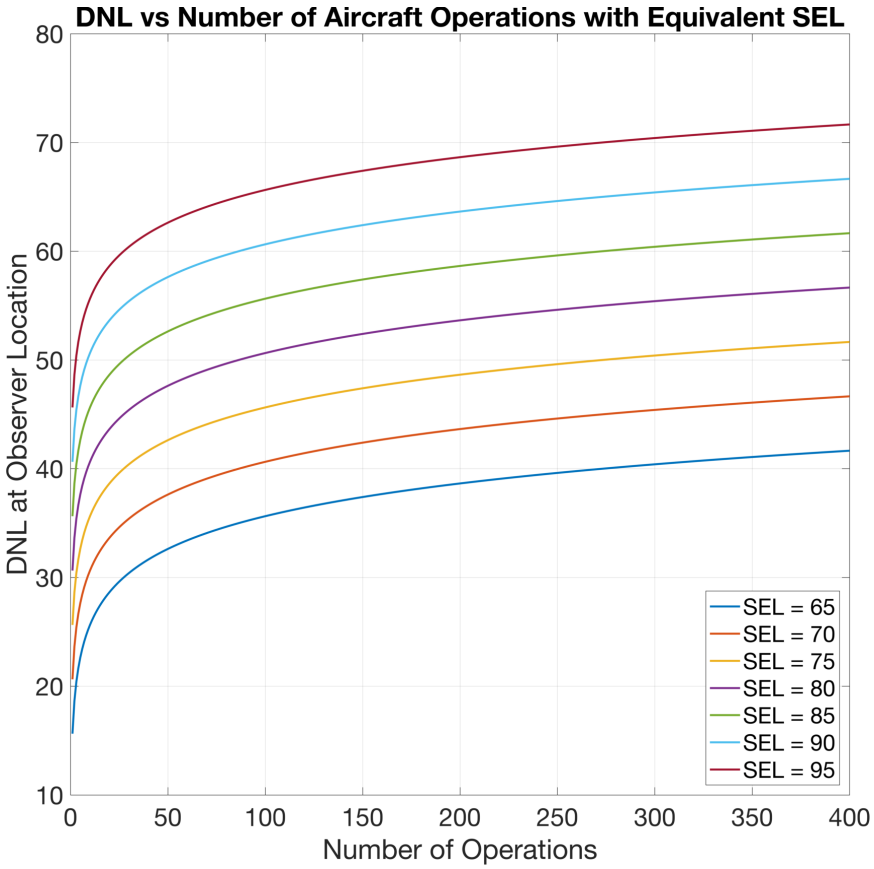

Figure 7: DNL vs. Number of Operations for Different SEL Values

In practice, DNL is often evaluated on an annualized basis. Since DNL typically requires analysis on a 24-hour time scale, this is accomplished by averaging total daily operations over the course of a year to obtain an annual average day of operations. While this allows for analysis using the standard DNL metric, the annual average day for which DNL is calculated does not actually represent a real day of operations but rather a fictitious day designed to reflect operational patterns on an annual basis. Since airports often utilize runways unequally on a day-to-day basis, as was explained in Chapter 1, this annual average day may therefore not effectively capture noise patterns actually experienced by communities on a typical day of operations over their neighborhood.

2.2.2.3 DNL and N_{above} in the Context of Annoyance

Communities often cite the repetitiveness of overflight noise, particularly with specific runway configurations, as a key factor in noise-related annoyance, particularly

for certain operational changes like the concentration of flight tracks on certain newer types of flight procedures [9]. Since N_{above} is directly related to the average frequency of overflights while DNL is not, N_{above} may better represent these operational changes in a manner consistent with the mechanisms through which communities are impacted by the noise from overflights.

2.3 U.S. Federal Airport Noise Regulation and Reporting

U.S. regulations governing aviation can be found in Title 14 of the Code of Federal Regulations (14 CFR). These regulations include rules that require assessment of noise impacts as a part of airport planning, which are enumerated in 14 CFR Part 150 [10] [11].

2.3.1 Use of DNL

In 14 CFR Part 150, DNL is identified as the primary metric for consistent noise exposure analysis for U.S. federal regulatory purposes [10]. In this Part, the lowest DNL threshold relevant for noise abatement or compatibility planning is 65dB DNL [10]. The study often cited as the basis for the 65dB significant noise threshold is discussed in Section 2.4 [12]. The continued validity of this metric and threshold as the basis for federally-mandated noise abatement is a topic of current and active discussion [12].

The U.S. National Environmental Policy Act (NEPA) provides additional guidance for aviation noise regulatory analysis using DNL. While 65dB DNL is considered the threshold for significant noise exposure by the FAA, NEPA analysis can require analysis at noise levels down to 45dB DNL [13]. This analysis creates no restrictions on implementation of procedures as the result of changes in population exposure at levels below 65dB DNL, however, as this analysis is required only for reporting purposes [13]. NEPA requires that changes only be reported if the change in noise exposure is greater than a certain threshold, which changes depending on the baseline noise level impacted [13]. A change must be greater than 5dB to need reporting between a 45dB and 60dB DNL baseline and greater than 3dB between 60dB and 65dB DNL [13].

2.3.2 Federally-Mandated Aviation Noise Analysis Tool: AEDT

14 CFR Part 150 also identifies a specific noise-modeling tool for use when conducting all analysis required by regulation. This was originally the Integrated Noise Model (INM), although INM has since been replaced by a successor, the FAA's Aviation Environmental Design Tool (AEDT) [6].

AEDT contains modules for analyzing aviation noise, fuel burn, and emissions at both the single flight and multi-flight levels [6]. The noise analysis module of AEDT leverages data from the AEDT fleet database, which includes data from the ICAO Aircraft Noise and Performance Database (ANP) and the Eurocontrol Base of Aircraft Data (BADA), to model aircraft performance in different phases of flight and to calculate noise [6]. AEDT noise calculations are based on data contained in noise-power-distance (NPD) curves, which provide noise levels in dB measured at different distances from a specific aircraft for different thrust settings and operational modes [6]. The operational modes include approach, departure, and level flight, to account for the fact that different sources of noise dominate in different phases of flight [6]. The NPD database directly includes curves for both SEL and $L_{A,max}$[5] and the methods in AEDT correct these curves for deviations due to factors including atmospheric attenuation, duration of exposure (for SEL only), and reflectivity off the ground [6]. As mentioned previously in Section 2.2.1, this means that SEL and $L_{A,max}$ are not computed directly from physics-based analysis of sound pressure level over time but rather from empirically-derived aircraft type-specific reference data sets for each metric.

2.4 Past Studies of Aviation Noise and Annoyance

Studies have been conducted over the years looking at human responses to aviation noise. One of these studies, by Schultz published in 1978 [14], is often cited in the context of describing the history of the use of DNL for regulatory purposes in the

[5] $L_{A,max}$ NPD data does not exist in AEDT for all aircraft. AEDT uses an empirical equation derived from aircraft with complete NPD data sets to calculate the equivalent $L_{A,max}$ NPD values from the SEL NPD data [6] but still does not necessarily equate them directly per the relationship depicted in Figure 5.

United States [12] The key element of the paper often used is a curve developed by Schultz based on data from a number of prior studies of noise and annoyance. This curve associates a percentage of respondents from each survey considered highly annoyed with the DNL levels at which they were exposed to the noise [14]. A version of this curve that also includes some more recent data points is shown in Figure 8.

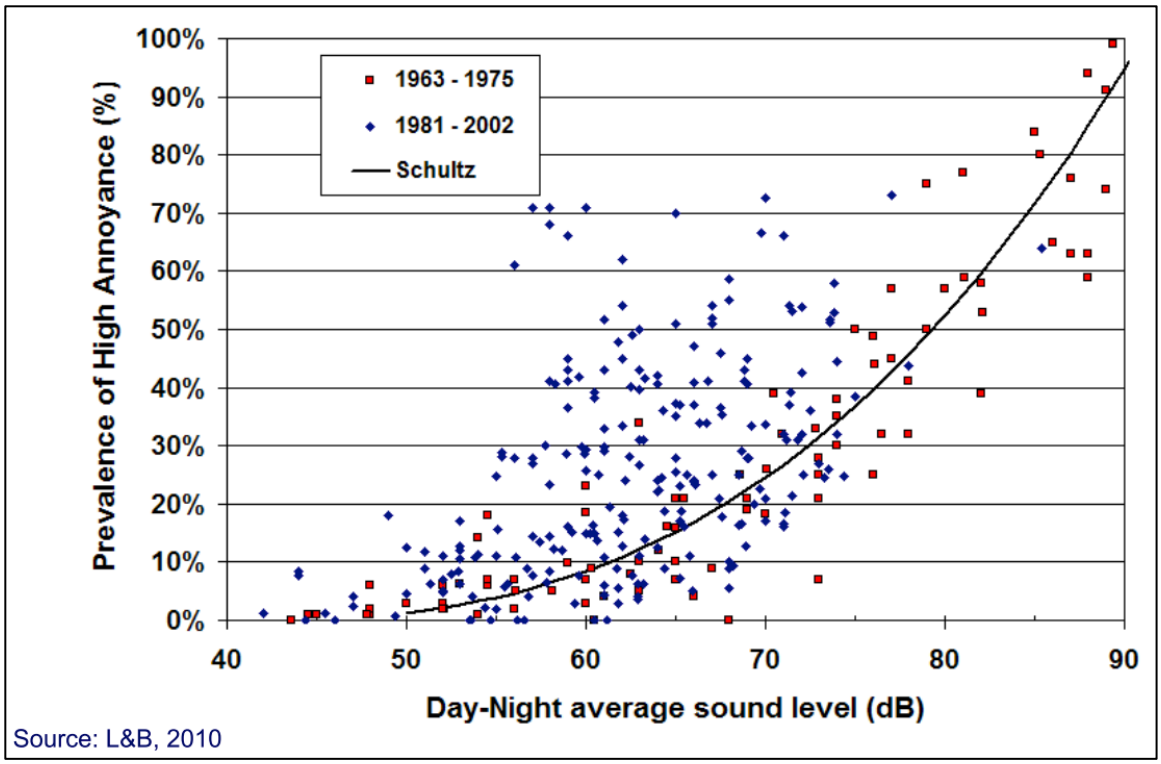

Figure 8: Percent of People Highly Annoyed by DNL. Source: HMMH [12]

Schultz found that a correlation existed between the median level of annoyance in an area and the noise level of that area, but no correlation between individual responses and noise level [14]. Interestingly, although Schultz's paper is often cited as part of the justification for the use of DNL as a regulatory metric [12], Schultz actually states in his paper that audibility of a noise event is probably more closely related to peak sound than time-averaged sound like DNL and that occurrences of individual noisy events are also likely important in understanding annoyance due to noise [14].

A more recent study published in 2014 looking at the impacts of aviation noise in terms of both annoyance and sleep disturbance found little correlation between

cumulative exposure metrics like DNL and levels of sleep disturbance [15], supporting Schultz's conclusion regarding maximum sound levels, DNL, and annoyance.

Page Intentionally Left Blank

Chapter 3 Overview of Case Studies

This thesis seeks to explore in a systematic manner the effectiveness with which different representative scenarios and noise metrics capture patterns of noise-related annoyance and potential community opposition to airport policy and procedure modifications. In order to do this, three different representative days of operations will be modeled. These three scenarios evaluated will be an annual average day, a representative day of heavy use of a specific departure runway, and a day representative of the hour of peak departures during this day. This modeled noise will then be compared with the number of noise complaint locations from a similar time period exposed to different levels of noise during a similar time period to assess the effectiveness by which analysis using each of these representative scenarios captures annoyance patterns.

As was introduced in Section 2.2.2.2, annual average day noise analysis is often used for understanding the aggregate impacts of airport operations on local communities. This annual average day, however, is fictitious as it reflects a full year of operations condensed to a daily timescale for noise impact analysis rather than representing an actual day of operations. This is due to the fact that airports often use particular runways and combinations of runways (called a runway configuration) unequally on a day-to-day basis based on wind direction or other operational or environmental factors [16]. Therefore, if a particular runway configuration is utilized for an extended period of time, the noise in particular locations during this time may differ substantially from that of the annual average day. This means that while the annual average day may reflect the time-averaged noise impacts on communities over the course of a year, it does not necessarily reflect the overflight patterns experienced by communities during the periods when they are impacted by noise. In other words, the annual average day averages out periods of heavy usage of particular runways with periods during which those runways are not used at all and will often show only moderate average noise impacts due to operations from that runway configuration. In some situations, even daily operations on a day of heavy usage of a single set of runways may not capture annoyance during the periods of peak operations during the day. Understanding the magnitude of these dilution effects is the primary motivation for comparing a day and hour of heavy usage of a particular runway

with an average annual day scenario. It is important to note that since these scenarios each specify a different total number of operations, the results will reflect both these different total numbers of operations and changing modeled runway use.

The airport used for these case studies will be Boston Logan International Airport (BOS). BOS was chosen as the airport of study due to the availability of both individual flight data and complaint data through ongoing work assessing noise impacts and potential mitigations at Boston Logan International Airport (BOS) in collaboration with Massport.[6] This complaint data, including a location for each complaint, comes from the records of calls made to the Massport noise complaint line and a web-based noise complaint form [17]. Given the available periods of complaint data and flight data, the case studies all use complaint data from August 2015-July 2016 and flight data from time periods in 2015 and 2016. This complaint data includes a total of 28,204 recorded complaints from 1,994 unique addresses. A map showing the locations of these noise complaints is given in Figure 9.

[6] Massport operates BOS, as well as Worcester Regional Airport and Hanscom Field.

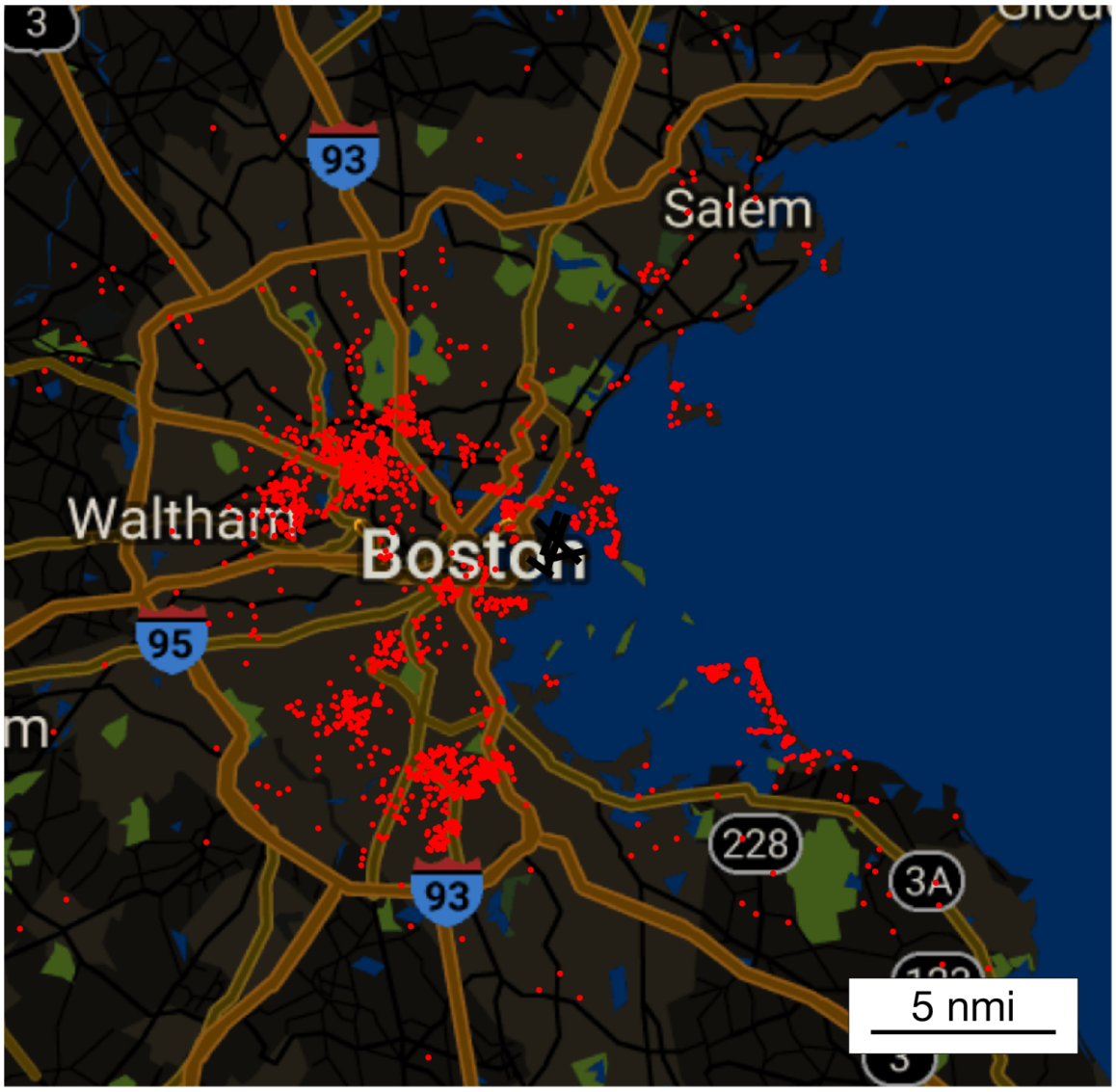

Figure 9: Locations of Noise Complaints at BOS, August 2015 – July 2016

Both DNL and N_{above} will be examined for each of these scenarios at a variety of noise levels. The effectiveness by which either multiple event noise metric captures annoyance as measured by number of people submitting complaints (number of complainants) will be measured using the methods outlined in Section 3.5. Details on the methods used for calculating the DNL and N_{above} noise impacts of each scenario can be found in Chapter 4.

For each case study, noise data is generated using a fleet of representative aircraft flying representative lateral tracks using case study-specific flight schedules. The

schedules for each case study are presented as part of the case study descriptions in Sections 3.1-3.3. To develop these schedules, analysis of flight records was conducted using a data set from the BOS-specific Noise and Operations Monitoring System (NOMS), which includes aircraft type, date, time of day, and runway used for each individual flight in 2015. Each of these schedules assigns flights to a particular runway, representative aircraft type, and time of day based on flight data for the time period of analysis for a scenario. Multiple aircraft types with similar characteristics are grouped into representative type bins, and all flights operated by aircraft in a particular bin are assigned to their representative aircraft type to develop the schedule for each scenario. The representative aircraft types used in this analysis are: the Boeing 777-300 (B773), the Airbus A320-212 (A320), the Boeing 737-800 (B738), the Boeing 757-200 (B752), the McDonnell Douglas MD-88 (MD88), the Embraer E-170LR (E170), and the Embraer E-145LR (E145). Further discussion of the selection of these representative types and the aircraft binning process can be found in Section 4.2.

3.1 Scenario 1: Annual Average Day

The first case study analysis will look at an overall average annual 2015 day at BOS. This analysis defines a representative single day by dividing total annual 2015 operations by 365 to generate a schedule representative of total annual operations that is on the 24-hour timescale appropriate for DNL analysis.

To develop the schedule for this case study, all flights in 2015 were grouped by type bin, runway used, operation type (arrival or departure), and time of day (day or night). The resulting allocation of departures by day and night is shown in Table 1 and Table 2, respectively, and the allocation of arrivals by day and night is shown in Table 3 and Table 4, respectively. Any operations assigned to runways with no assigned tracks for that operation type are excluded from analysis; however, this only occurs for a very small number of operations and is expected to have had a negligible impact on results.

Table 1: Annual Average Day Departures Per Runway by Aircraft Type Bin - Day

Representative Aircraft Type	15R	04R	04L	09	14	15L	33L	22L	22R	27	32	33R
B773	2.37	1.89		1.82			3.05	1.53	3.38	0.47		
A320	3.35	5.52		28.15			16.68	3.19	31.64	11.38		
B738	2.75	6.35		18.02			11.65	3.43	21.42	6.65		
B752	0.54	0.84		4.46			2.63	0.25	5.17	1.48		
MD88	0.35	0.31		6.59			2.66	0.07	6.65	3.00		
E170	1.68	1.09		37.02			14.29	0.10	37.26	14.65		
E145	0.64	1.54	5.95	16.72			9.80	0.06	22.72	5.47	0.01	0.01

Table 2: Annual Average Day Departures Per Runway by Aircraft Type Bin - Night

Representative Aircraft Type	15R	04R	04L	09	14	15L	33L	22L	22R	27	32	33R
B773	2.35	0.44		0.73			2.20	0.32	1.91	0.08		
A320	2.90	0.55		2.56			2.07	0.24	3.61	2.68		
B738	3.35	0.83		2.16			2.00	0.41	3.25	2.58		
B752	0.45	0.13		0.51			0.44	0.06	0.86	0.41		
MD88	0.53	0.09		0.85			0.70	0.02	1.31	0.59		
E170	1.37	0.23		3.11			0.96	0.02	4.01	3.25		
E145	0.69	0.10	0.21	0.49			0.78	0.02	1.03	0.33		

Table 3: Annual Average Day Arrivals Per Runway by Aircraft Type Bin - Day

Representative Aircraft Type	15R	04R	04L	09	14	15L	33L	22L	22R	27	32	33R
B773	0.39	8.10	0.06				3.57	6.07		3.09		
A320	1.22	28.48	3.29				12.06	21.45	0.02	22.20		
B738	0.88	21.62	1.67				7.13	11.32	0.01	20.03		
B752	0.24	5.37	0.22				1.62	3.18		4.02		
MD88	0.28	6.39	0.73				3.01	3.60		6.08		
E170	1.52	32.61	6.46				16.24	24.24	0.04	27.05	2.67	0.01
E145	0.75	10.94	12.51				7.94	16.85	0.53	10.33	4.34	0.14

Table 4: Annual Average Day Arrivals Per Runway by Aircraft Type Bin - Night

Representative Aircraft Type	15R	04R	04L	09	14	15L	33L	22L	22R	27	32	33R
B773												
A320	0.58	5.26	0.06				7.81	9.93		3.35		
B738	0.48	4.21					7.85	7.85		2.77		
B752	0.08	0.67	0.01				1.14	1.29		0.43		
MD88	0.07	0.90					1.57	1.31		0.48		
E170	0.33	2.48	0.06				2.36	4.48		1.89		
E145	0.08	0.80					1.11	1.42		0.45	0.01	0.01

3.2 Scenario 2: 33L Peak Day

The second case study will model operations for the specific day in 2015 with the highest number of departures from runway 33L, which was July 22, 2015. On this day, a total of 77% of departure operations used this runway. In this situation, the people under the flight tracks from this heavily utilized runway will be subjected to a larger number of operations and likely exposed to higher noise levels than are reflected in the annual average day of Scenario 1. This scenario attempts to demonstrate the effects of the dilution of specific runway usage patterns in the annual average day analysis relative to the actual noise impacts seen on a day-to-day basis. A diagram of the layout of the airport at BOS highlighting the location and direction of runway 33L departures is shown in Figure 10.

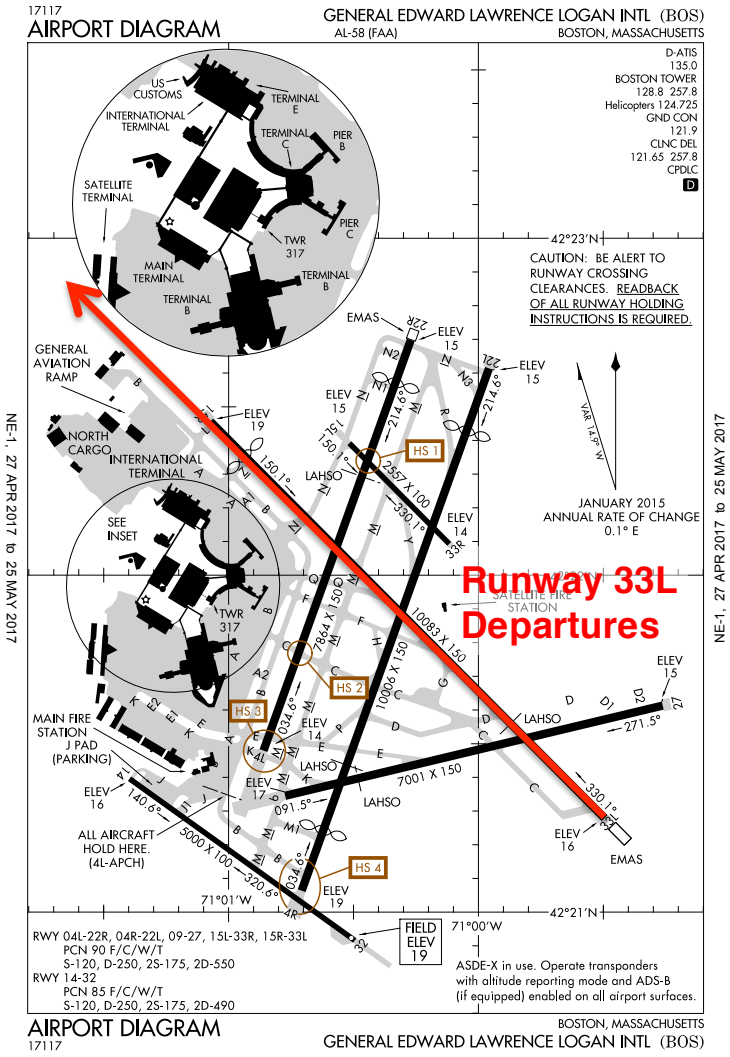

Figure 10: FAA Airport Diagram for BOS with Annotation For Runway 33L Departures. Airport Diagram Source: FAA [18]

Runway 33L was selected as the focal point for this analysis for two primary reasons. First, there is a clear subset of noise complaints surrounding these flight tracks, which allows for evaluation of noise impact metrics using a set of complaints filtered to be attributable to the specific operational scenario analyzed. These noise complaints, along with a large number of departure tracks from BOS, are shown in Figure 11. Second, since communities under this flight path experienced a clear change in flight track concentration with the implementation of PBN procedures (Figure 1) this particular flight

track is of interest in understanding the noise impact of the concentration of flight tracks on PBN procedures.

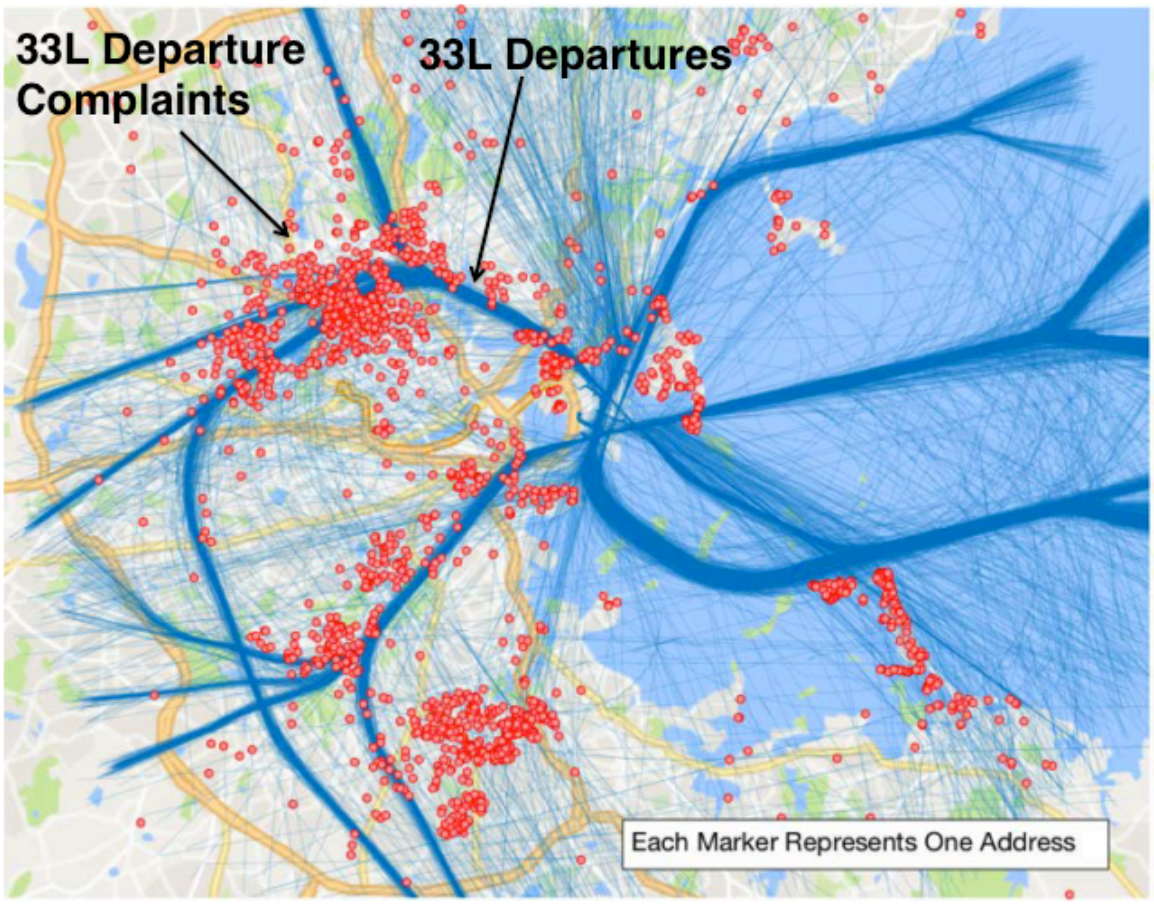

Figure 11: BOS Runway 33L Departures and Complaints. Source: Hansman [2]

Since this case study models a high percentage of flights departing from runway 33L, the noise impacts of this case study will be evaluated against only complaints likely to be related to runway 33L departures. For this filtering of complainant data, relevant complainant locations were considered to be those located in the northwest quadrant from the airport. These complainants are highlighted in Figure 12. The use of this criterion is justified by the fact that the portions of the tracks from this runway likely to contribute to noise exposure fall in this quadrant and the majority of complainants surrounding these tracks lie in this quadrant.

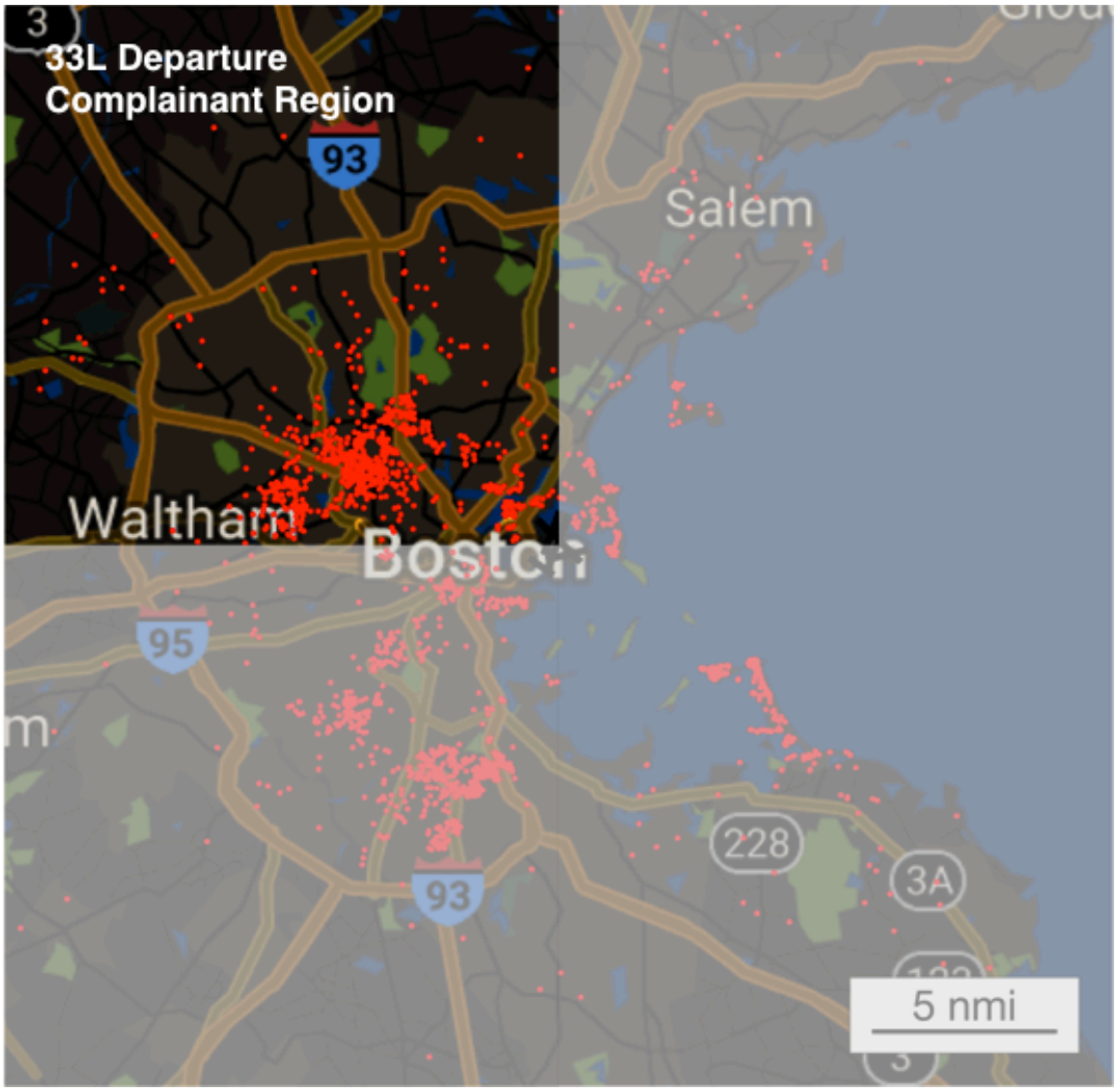

Figure 12: Northwest Quadrant Complainants at BOS, August 2015 – July 2016

To develop the schedule for this case study, all flights on July 22, 2015 were grouped by type bin, runway used, operation type (arrival or departure), and time of day (day or night). Flight allocation for this analysis is shown for departures by day and night in Table 5 and Table 6, respectively, and for arrivals by day and night in Table 7 and Table 8, respectively. These show almost all departures from runways 33L and 27 and almost all arrivals to runways 33L, 27, and 32 on that date, which is consistent with one of the primary runway configurations at BOS [16]. It is important to note that this peak day schedule has 18% more total operations and 27% more nighttime operations than the

annual average day scenario (1072 vs. 908 total and 174 vs. 137 nighttime), which contributes to overall higher relative noise exposure from this scenario.

Table 5: 33L Peak Day Departures Per Runway by Aircraft Type Bin - Day

Representative Aircraft Type	15R	04R	04L	09	14	15L	33L	22L	22R	27	32	33R
B773												
A320												
B738												
B752												
MD88												
E170												
E145												

Table 6: 33L Peak Day Departures Per Runway by Aircraft Type Bin - Night

Representative Aircraft Type	15R	04R	04L	09	14	15L	33L	22L	22R	27	32	33R
B773												
A320												
B738												
B752												
MD88												
E170												
E145												

Table 7: 33L Peak Day Arrivals Per Runway by Aircraft Type Bin - Day

Representative Aircraft Type	15R	04R	04L	09	14	15L	33L	22L	22R	27	32	33R
B773							15			11		
A320							12			79		
B738							10			69		
B752							2			11		
MD88							3			21		
E170							17			91	20	
E145							15			12	49	1

Table 8: 33L Peak Day Arrivals Per Runway by Aircraft Type Bin - Night

Representative Aircraft Type	15R	04R	04L	09	14	15L	33L	22L	22R	27	32	33R
B773												
A320							22			14		
B738							18			14		
B752							2					
MD88							5			3		
E170							7			6		
E145							6			1		

3.3 Scenario 3: 33L Peak Hour

The final operational scenario analysis will look at the peak hour of departures on the 33L peak day. For this peak hour analysis, the number of operations during the hour will be scaled up to a full day of operations, with each hour of the day assigned the number of operations during the peak hour, so that all quantitative results are directly comparable to the results from the annual average day and peak day analyses. This scenario attempts to provide a further demonstration of the dilution in noise impact that arises from looking at noise impacts over larger time scales. This scenario will also use the filtered complainant data set described for the 33L peak day scenario.

Additional data sources were required to develop the schedule for this scenario, as exact time of departure or arrival was not available in the NOMS data. The FAA's public Aviation System Performance Metrics (ASPM) system [19] was used to fill this gap and obtain the number of operations per hour for the day of interest. According to the ASPM daily report for BOS operations on July 22, 2015, the peak hour of departures was during the daytime hour from 5pm-6pm, with a total of 31 arrivals and 48 departures during that period. Based on the NOMS data, there were a total of 438 daytime arrivals and 460 daytime departures on that date in the non-excluded bins; the ASPM hourly operations report includes 443 daytime arrivals and 493 daytime departures on that date. Since the total number of operations counted by the two data sources were not identical, the total number of hourly operations used in this analysis are a fraction of total NOMS daytime

operations equivalent to the fraction of total ASPM daytime operations. Applying this correction yields a final number of roughly 30.65 arrivals and 44.79 departures during the peak departure hour.

To calculate results on the same time scale basis as used for the annual average and 33L peak day scenarios these hourly operations were then scaled to a full 24-hour day. The schedule for this 33L peak hour analysis maintains the same distribution of flights amongst runways and representative aircraft bins from the 33L peak day daytime arrivals and departures for each of these 24 hours. 15 hours' worth of flights are assigned as daytime flights (7am-10pm) and the remaining 9 hours of flights are assigned as nighttime flights. It is important to note that this peak hour schedule has approximately twice as many total operations and five times as many nighttime operations compared to the annual average day scenario (1810 vs. 908 total and 679 vs. 137 nighttime). This contributes to substantially higher overall noise exposure from this scenario.

Table 9: 33L Peak Hour Departures Per Runway by Aircraft Type Bin - Day

Representative Aircraft Type	15R	04R	04L	09	14	15L	33L	22L	22R	27	32	33R
B773												
A320							127.06			27.75		
B738							112.45			20.45		
B752							16.06			5.84		
MD88							29.21			8.76		
E170							151.89			30.67		
E145		8.76					96.39			13.14		

Table 10: 33L Peak Hour Departures Per Runway by Aircraft Type Bin - Night

Representative Aircraft Type	15R	04R	04L	09	14	15L	33L	22L	22R	27	32	33R
B773							13.14			0.88		
A320							76.24			16.65		
B738							67.47			12.27		
B752							9.64			3.51		
MD88							17.53			5.26		
E170							91.13			18.40		
E145		5.26					57.83			7.89		

Table 11: 33L Peak Hour Arrivals Per Runway by Aircraft Type Bin - Day

Representative Aircraft Type	15R	04R	04L	09	14	15L	33L	22L	22R	27	32	33R
B773							15.74					
A320							12.60					
B738							10.50					
B752							2.10					
MD88							3.15					
E170							17.84				20.99	
E145							15.74				51.43	1.05

Table 12: 33L Peak Hour Arrivals Per Runway by Aircraft Type Bin - Night

Representative Aircraft Type	15R	04R	04L	09	14	15L	33L	22L	22R	27	32	33R
B773							9.45			6.93		
A320							7.56			49.75		
B738							6.30			43.46		
B752							1.26			6.93		
MD88							1.89			13.23		
E170							10.71			57.31	12.60	
E145							9.45			7.56	30.86	0.63

3.4 Quantification of Scenario Noise Impact: DNL and N_{above}

Using methodology outlined in Chapter 4, DNL and N_{above} impacts results will be calculated for each scenario. These noise impact results will be examined over a wide range of DNL levels and N_{above} noise level and overflight count thresholds.

The DNL thresholds were selected based on the levels referenced in U.S. regulatory noise policy. As the lowest level discussed for which an increase in noise might be considered significant is 45dB (see Section 2.3.1) and the level at which baseline noise exposure is considered significant is 65dB, DNL contours will be examined from 45dB to 65dB in 5dB increments.

N_{above} $L_{A,max}$ thresholds will be examined from 55dB to 70dB for daytime flights, again in 5dB increments, to cover noise levels above that roughly comparable to average conversation (see Figure 4) through those included in previous analyses [13]. The threshold for nighttime flights will be 10dB lower than the corresponding daytime threshold. For each of these $L_{A,max}$ thresholds, contours will be examined for 25, 50, 100, 250, and 500 number of overflights with $L_{A,max}$ above the threshold. 25 overflights correspond to an average of roughly 1 flight per hour, 50 overflights correspond to roughly 1 flight every half hour, 100 overflights correspond to roughly 1 flight every quarter hour, 250 overflights correspond to roughly 1 flight every 6 minutes, and 500 overflights correspond to roughly 1 flight every 3 minutes.

3.5 Evaluation of the Effectiveness of Noise Impact Metrics with Respect to Complainant Location

DNL and N_{above} results are calculated as exposure levels over a grid of observer locations. Using the grid points exposed at different noise and overflight levels, contours can then be defined surrounding regions of exposure at specific levels[7]. The quantitative comparisons presented in Chapter 6 use a series of metrics defined based on the shape

[7] These contours are defined as polygons. Contour area and coverage comparisons were calculated using built-in Matlab polygon functions [26] [27].

and coverage of each of these contours. These are: contour area, population exposure, and percent of complainants contained within the contour.

Metrics related to both contour area and population exposure are included in the results for completeness, as contour area is more generalizable to airports with different surrounding population patterns. However, results will also include population exposure and complainant address coverage metrics as this particular analysis is specific to BOS and the fact that a substantial portion of the area surrounding BOS is covered by water gives the location distinctive population characteristics. The methodology used to calculate the results for population exposure and complainant coverage are outlined in the following subsections.

3.5.1 Calculation of Population Exposure

A grid of population densities was generated for the regions surrounding a number of U.S. airports, including BOS.[8] These were generated from 2010 census data, which was re-gridded into 0.1nmi square segments. The population from each of these grid squares was then associated with the centroid of that grid square, generating a 0.1nmi-spaced grid of population counts. The populations located at points within a contour are considered exposed to that contour.

3.5.2 Calculation of Complainant Coverage

Noise complaint records from BOS for the 12-month period from August 2015-July 2016 were used for this analysis. This complaint data, including a street address for each complaint, originates from the records of calls made to the Massport noise complaint line and a web-based noise complaint form [17] and includes a total of 28,204 recorded complaints from 1,994 unique addresses. It is important to note that while complaint patterns likely identify hotspots of perceived noise impact, complaints, by their nature, are self-disclosed and individual complaints may not directly reflect general

[8] These population grids were created as part of prior work by Luke Jensen and used for this analysis with permission.

adverse noise impact. A map showing the locations of these noise complaints is given in Figure 9.

Individual complainants were identified from this data by their unique addresses, and these addresses were converted to latitude and longitude coordinates (geocoded) using Google's geocoding API [20]. All but six complainant addresses were automatically geocoded using the address information provided by complainants. Of the remainder, all but one were able to be associated with a valid address manually and geocoded using the Google API. The final address is excluded from analysis, resulting in 1,993 successfully geocoded addresses. All complainant addresses outside a 58nmi-bounding box surrounding the airport were excluded.[9] Slightly over 1% of valid complainants fall outside this box, resulting in a total of 1,970 complainants used as the basis for computation of percentage of complainants contained within a contour. For the analyses in Scenarios 2 and 3 requiring filtering of complainant data for complaints related to 33L departures, 832 of these filtered complainants lie in the northwest quadrant and are used as the basis for calculating percentage of complainants contained in the contours for these scenarios.

Each remaining complainant location included within a contour was considered contained by that contour. The percentage of complainants covered by a contour was then calculated using the number of complainants contained by the contour and the total number of complainants included for the scenario.

[9] This was done primarily for consistency with the extent of the noise grids modeled.

Chapter 4 Noise Modeling Methodology

This thesis uses tools developed by a team at MIT, including the author and others, to generate quantitative noise results for use in comparing potential methods of interest for conducting noise analysis. This section will provide an overview of the framework for aviation environmental impacts analysis used for the case studies in this thesis and will provide a detailed explanation for the methodology used to generate the specific results presented in this thesis. This is important for understanding the scope of applicability of the results presented and for potential comparison with other environmental impact analyses.

4.1 Rapid Aviation Environmental Impact Modeling Framework Overview

A tool has been developed for rapid analysis of aviation environmental impacts to enable broader analysis of both high-level policy changes and specific changes in airport arrival and departure procedures [21]. This framework was designed to enable rapid airport-level and national-level environmental impacts analysis. An overview of the framework as applied to this thesis is shown in Figure 13.

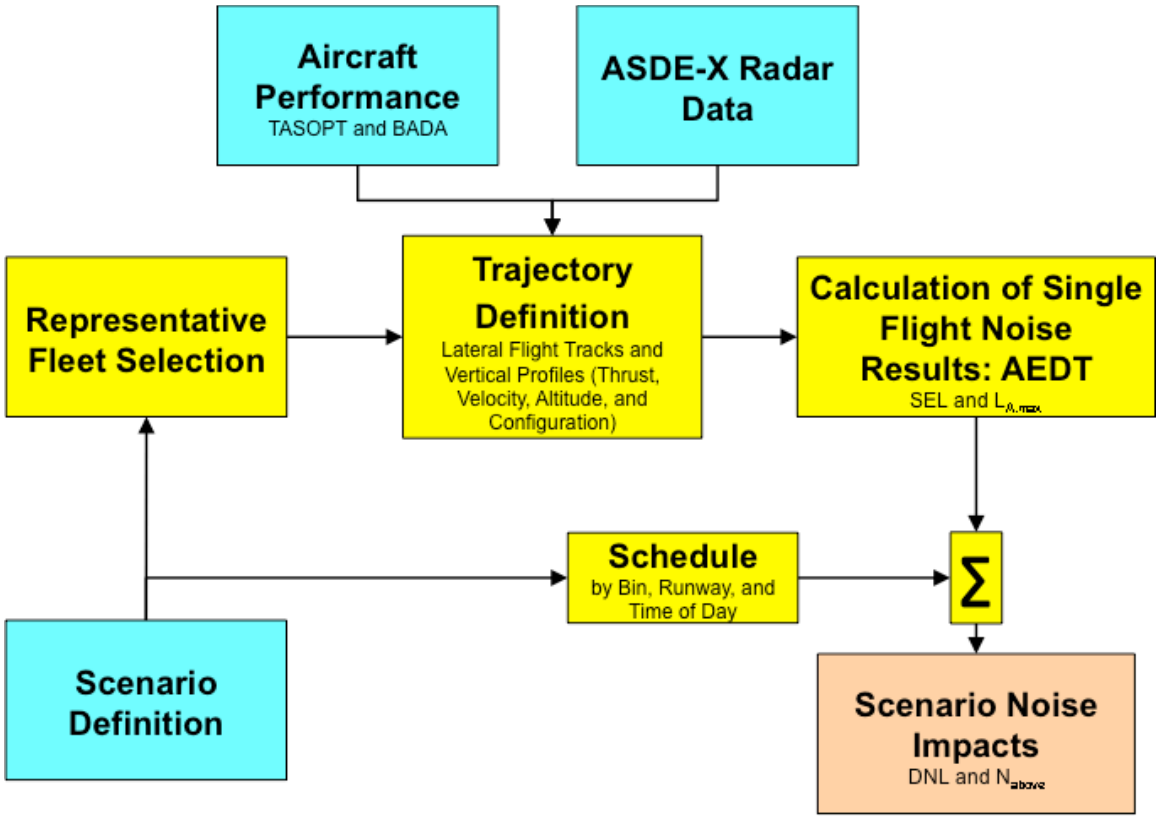

Figure 13: Diagram of Rapid Aviation Environmental Modeling Toolset. Adapted from [21]

The framework outlines a toolset that calculates total noise for a scenario using:

- a representative fleet model,
- a trajectory for each representative flight, including
    - representative lateral tracks, and
    - a vertical flight profile, including altitude, speed, thrust, and configuration as a function of ground track distance for each aircraft type of interest, and
- a representative schedule, including runway and track assignment by aircraft type by time of day.

First, a full trajectory is calculated for each representative flight. A representative flight is a combination of aircraft type (and corresponding reference vertical profile) and lateral trajectory. Then, each of these flights are run through a noise model to calculate the noise impact, in this thesis SEL and $L_{A,max}$, at defined observer grid locations. The

grid data for the individual flights in each scenario is then combined with a schedule and summed to calculate a scenario aggregate result noise impact grid.

The methods used to develop the representative fleet model, representative lateral tracks, and vertical profiles used to as inputs for generating the single flight noise results are outlined in Sections 4.2, 4.3.1, and 4.3.2, respectively. Section 4.4 discusses the process used to calculate single flight noise impact results from these components. The schedules used for each case study were previously outlined in Sections 3.1-3.3.

4.2 Representative Fleet Selection

Since the analysis in this thesis is focused around BOS, a set of aircraft types generally representative of the aircraft categories operating at that airport was desired. This representative fleet includes the following: a twin-aisle jet (TA), a set of single-aisle jets, an older jet (OJ), a large regional jet (LRJ), and a small regional jet (SRJ). Due to the availability of additional previously modeled aircraft types in the single aisle category, additional fidelity is added by separately modeling the larger Boeing 757 family (B757) and the smaller Boeing 737 (B737) and Airbus A320 families. The full representative fleet selected is shown in Table 13.

Table 13: Fleet Selection and Daily Operations Counts

Representative Aircraft Type	Category Name	Category Description
B773		
A320	B757	Boeing 757 Family
B738	A320	
B752	B737	Boeing 737 Family
MD88	OJ	
E170	LRJ	Large Regional Jet
E145	SRJ	
--	PNJ UNK	Excluded (Piston Engine and Unknown)

After these representative aircraft types were selected, each flight was assigned to one of the representative aircraft types by grouping the aircraft types for each flight into individual bins. The full assignment of aircraft types to their respective bins is shown in Appendix A. Due to modeling constraints related to non-turbojet aircraft, all piston-engine, helicopter, and aircraft with unidentified types were excluded from analysis. All business jets and turboprop aircraft were grouped with the small regional jet category.

Excluded aircraft account for roughly 10% of all operations. Excluding these flights is justified for two reasons: 1) since the type of aircraft is sufficiently different from a modeled aircraft type so as to make noise impact modeling less believable, and 2) since some of these aircraft do not fly on published procedures the flight tracks of some number of flights are unlikely to fit the representative lateral track clusters and should therefore be excluded from the modeling.

4.3 Trajectory Definition

4.3.1 Lateral Track Generation and Runway Assignment

Representative lateral tracks were selected based on a clustering of radar track data. Flights are organized into clusters using a clustering algorithm, centroids are defined for each cluster, and the flight track in each cluster with the smallest RMS distance to the centroid is selected as the representative ground track for that cluster.[10] For this analysis, the clustering was done using ASDE-X radar data from 20 days of operations from April 2015 through March 2016. As lateral track is unlikely to be substantially influenced by aircraft type, the clustering was done on all flights regardless of representative type bin. Additional filtering was done on these clusters to eliminate any with less than 10 tracks assigned to the cluster. This resulted in a total of 19 representative departure tracks and 10 representative arrival tracks, with approximately 84% of arrivals and approximately 91% of departures assigned to clusters. All of the

[10] For this analysis, part of the existing rapid modeling toolset written by Callen Brooks was used. Further information regarding the clustering methodology can be found in [21] and [28].

trajectories used for the clustering are shown in Figure 14, with non-conforming (tracks not assigned to a cluster) shown in light gray. Centroids and representative tracks for each of these clusters are shown in Figure 15, and cluster membership (the number of flights in each cluster and color assignment of clusters by number) is shown in Figure 16.

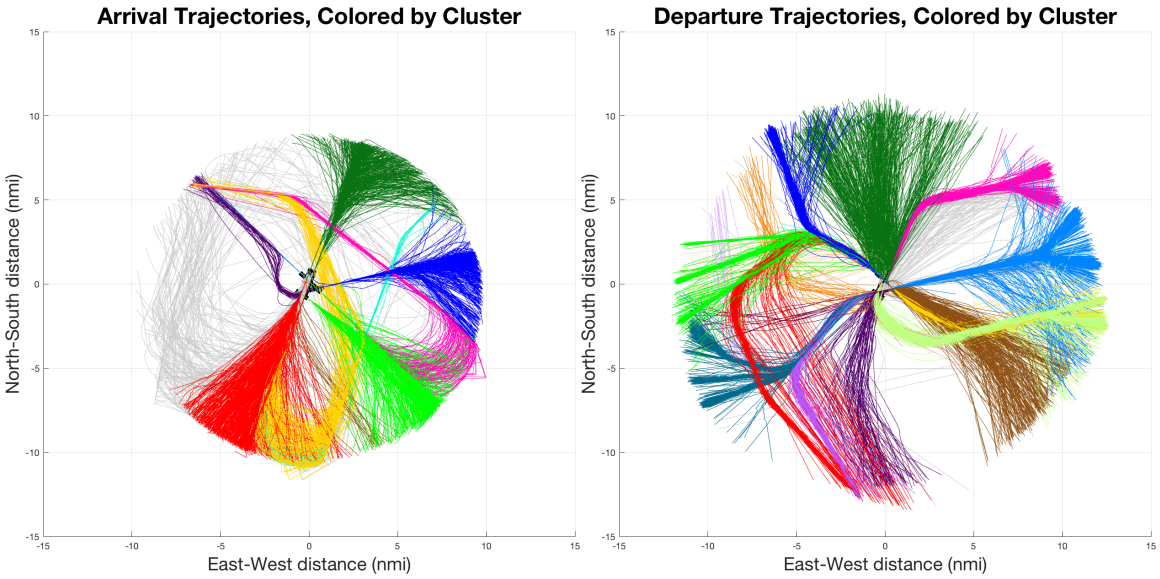

Figure 14: Clusters of Arrival (left) and Departure (right) Tracks at BOS from 20 days of ASDE-X data 2015-2016

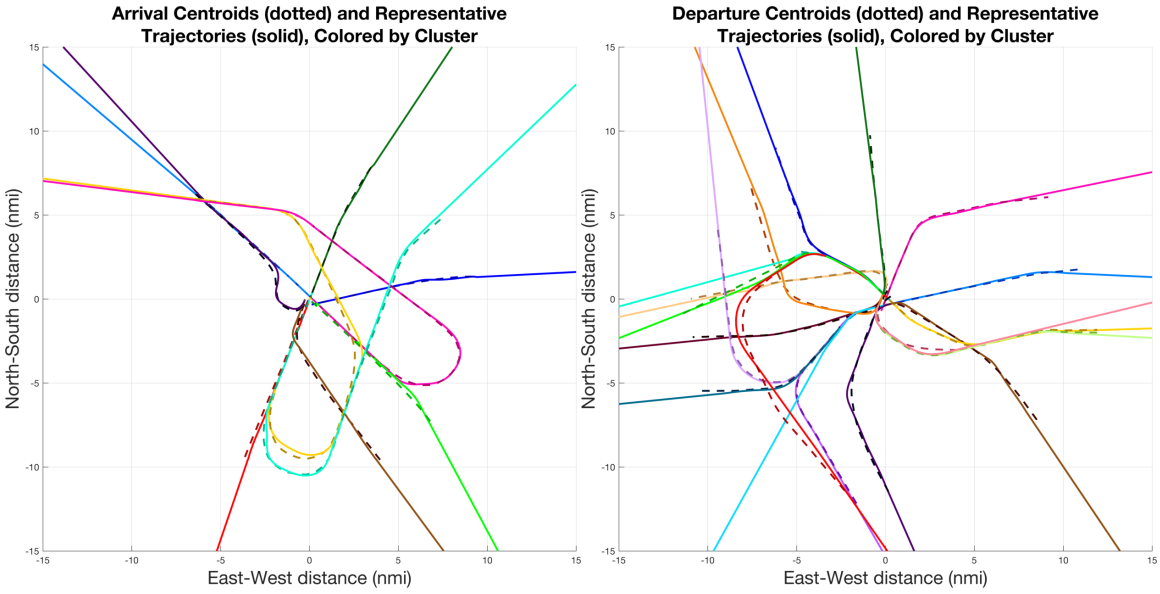

Figure 15: Centroids and Representative Tracks for Arrival (left) and Departure (right) Clusters

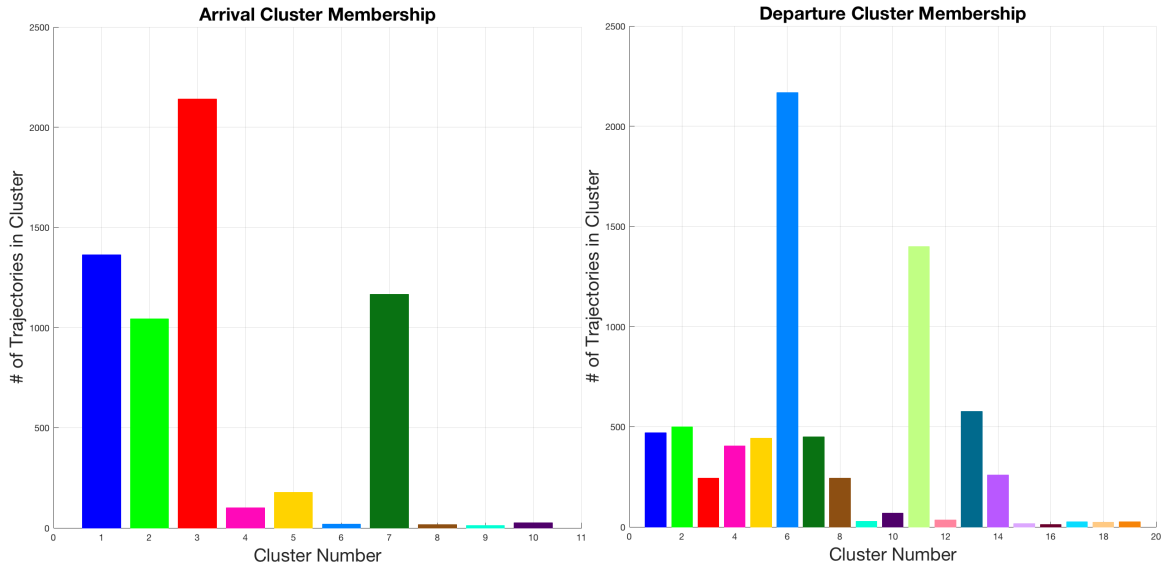

Figure 16: Arrival (left) and Departure (right) Cluster Membership

Although each representative track is by definition assigned to only a single runway, the flights in a cluster may originate or terminate on multiple runways since the tracks are likely to include many more points away from the airport than on the airport surface or immediately after takeoff or before landing. Additionally, flights to or from a particular runway are often included in multiple clusters depending on the incoming or outgoing flight path or direction. Therefore, additional analysis was done to proportionally assign flights on a given runway to each of the tracks with flights on that runway.

A runway detection algorithm was used on all flights in each cluster to find the number of flights on a given runway in each cluster. This algorithm checked the terminal point of the radar track against a line drawn between the two runway end points and the average heading between the two sets of terminal track points against the expected runway heading based on the runway end points. Runway location data was retrieved from AirNav [22]. If no runway was sufficiently close to a track by both conditions,[11] the

[11] Points along the runway were sampled at 200-foot spacing. A distance match was declared for a track terminal point within a 350-foot buffer around this line of points (more specifically, within $\sqrt{200^2 + 350^2}$ feet of a sample point). A heading match was considered to be an average between the terminal two sets of track points within 45° of the calculated runway heading.

runway was left unassigned for that track. Both of these conditions were enforced to limit poor assignment due to erroneous track data. Using this algorithm, an average of approximately 1% of flights were left unassigned in each cluster, with a maximum of under 6% for one arrival cluster and some clusters with no unassigned tracks. These numbers of flights were then used to allocate a given runway's flights to the representative tracks.[12] The final percentages of flights on each runway allocated to a given cluster for arrivals are shown in Table 14 and for departures are shown in Table 15, respectively.

Table 14: Track Allocation by Runway – Arrivals

Cluster #	15R	04R	04L	09	14	15L	33L	22L	22R	27	32	33R
1												
2							89.5%			0.1%	100%	
3		89.4%	92.4%									
4							10.5%					
5		9.8%	1.1%									
6	100%											
7								100%	100%			
8		0.2%	2.3%									
9		0.6%	0.2%									
10			4.1%									

[12] Each cluster was manually checked after processing through the runway detection algorithm to ensure that all runways to which at least one flight was assigned by the algorithm actually had flights originating or terminating on that runway. This resulted in manual corrections for arrival cluster percentages for runway 14, which actually had no flights arriving on the runway in any cluster, and runway 22L, which actually had no arrivals in cluster 3. These corrections should have minimal impact on results, however, due to the low number of flights assigned to runway 14 (a total of one) and the low percentage of flights corrected on runway 22L (<0.25%).

Table 15: Track Allocation by Runway – Departures

Cluster #	15R	04R	04L	09	14	15L	33L	22L	22R	27	32	33R
1												
2												
3												
4												
5	98.9%											
6												
7												
8	0.7%											
9												
10												
11												
12												
13												
14												
15												
16												
17												
18												
19	0.5%											

4.3.2 Vertical Profile Definition

Vertical profiles – including altitude, speed, and thrust as a function of ground track distance – for each representative aircraft type were defined using a physics-based profile generator.[13] For both arrivals and departures, the profiles were designed such that altitude as a function of ground track distance closely matched those seen in actual ASDE-X radar profiles at BOS. For both arrivals and departures, a ground track point of zero corresponds to the threshold of the runway end number used (i.e. both an arrival and a departure from runway 33L would have the zero point at the threshold nearest the painted "33L"). Arrival and departure profiles are defined somewhat differently, however, and the matching procedure for each is described separately in the following two subsections. A single reference profile for each representative type is defined for each operation type (arrival or departure), and the points along each reference lateral track are

[13] This was originally developed by Jacqueline Thomas and modified for this analysis. Additional details on the original version of this profile generator can be found in [23].

then interpolated to the ground track path lengths in this reference profile for each aircraft type.

Two aircraft performance models are employed for different performance parameters required for profile calculation. The first is Eurocontrol's Base of Aircraft DAta version 4 (BADA 4), which contains a large number of performance parameters for existing aircraft types. BADA4 is used as the source for flap extension speeds and drag for each configuration as well as climb and descent speeds for the portion of the profile above 10000'. The second is the Transport Aircraft System OPTimization (TASOPT). Unlike BADA, TASOPT is an aircraft design tool, used in this context to create aircraft that match the geometry and mission profiles of existing aircraft types. Although TASOPT aircraft are not identical to the actual aircraft, these modeled aircraft are used as a source for parameters not currently taken from BADA, including approach speed (V_{app}), V_2, and the parameters for calculating climb thrust lapse with altitude.

4.3.2.1 Arrivals

Given that many arrivals use standard instrument approach procedures, which typically use a 3-degree glideslope to the runway, representative arrival profiles follow a generally 3-degree glideslope to touchdown over the ground track ranges of focus for noise analysis. As aircraft typically do not land exactly on the runway threshold, the ASDE-X radar data used for the clustering described in Section 4.3.1 was examined. The threshold-aligned clustered altitude profiles for Boeing 737-800 (B738) arrivals are shown in Figure 17.

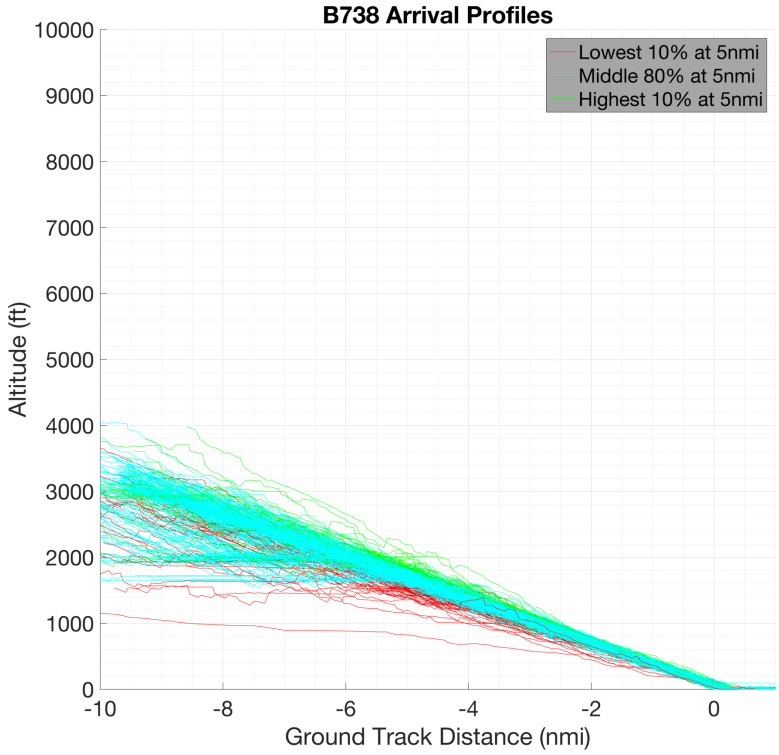

Figure 17: Arrival Profile Altitudes from 20 days of ASDE-X data for the Boeing 737-800

For each representative aircraft type, the touchdown point relative to the threshold was calculated for each radar trajectory. Touchdown was defined as the first radar point with an altitude within 20 feet of the minimum altitude of the trajectory, and the threshold was defined by a line perpendicular to the runway centerline through the latitude-longitude point of the relevant runway threshold. The touchdown point for each representative aircraft type was then set to the median of these touchdown points.[14] A median landing roll distance was similarly calculated for each representative aircraft type as the median path length from each trajectory's touchdown point to the terminal point of its landing roll. As each radar track was previously truncated to exclude points with under 60 knots of ground speed, this landing roll corresponds to the portion of the landing roll during which the aircraft decelerates from touchdown speed to 60 knots ground speed.

[14] For this analysis, only flights assigned to a cluster that were also detected as on the same runway as the representative trajectory for that cluster were included.

Table 16 summarizes the parameters used to define each segment of the arrival profiles, where altitude as a function of ground track distance is prescribed by the glidepath angle on each segment. Speed brakes are excluded from the analysis in this paper, so profiles may have thrust values below those physically possible for the aircraft type in order to maintain glideslope. The profile begins with a 2.5° glideslope from 20000' to 5000'. This angle is used to better model deceleration across the fleet as some aircraft have difficulty decelerating while on a 3° glideslope. Throughout the trajectory, thrust is set as necessary to achieve the required altitude and speed with the prescribed configuration and glide slope. $V_{descent}$ is the aircraft-specific BADA4-prescribed descent angle above 10000' and $V_{approach}$ is the aircraft-specific approach speed from TASOPT. For each aircraft type, configuration (flap and gear) changes are defined to occur at 15 knots indicated airspeed (KIAS) below the maximum flaps extended speed for that configuration, as defined by BADA4. Modeled aircraft have various numbers of possible flap settings, so to model all aircraft consistently, the first flap transition points are prescribed relative to the number of settings between clean and full. Three flap transitions are defined to occur between clean and the last setting before full; for aircraft with fewer than six flap settings only the first one or two of these transitions will occur and the other segments will be pure descent segments. At 1500', all aircraft extend landing gear and go to the last flap setting before full; at 1000' aircraft deploy full flaps.

Table 16: Approach Profile Definition. Adapted and Updated from [23]

Altitude (ft)	Speed (kts IAS)	Configuration	Glideslope	Thrust
[20000, 11000]	$V_{descent}$	Clean	2.5°	As required to maintain glideslope
[11000, 10000]	[$V_{descent}$, 250]	Clean	2.5°	As required to maintain glideslope
[10000, 6000]	250	Clean	2.5°	As required to maintain glideslope
[6000, 5000]	[250, $V_{1/4flap}$ -15]	Clean	2.5°	As required to maintain glideslope
[5000, 4000]	[$V_{1/4flap}$ -15, $V_{1/2flap}$ -15]	Flaps 1/4 between clean and full-1	3°	As required to maintain glideslope
[4000, 3000]	[$V_{1/2flap}$ -15, $V_{approach}$+30]	Flaps 1/2 between clean and full-1	3°	As required to maintain glideslope
[3000, 1500]	[$V_{approach}$+30, $V_{approach}$]	Flaps 3/4 between clean and full-1	3°	As required to maintain glideslope
[1500, 1000]	$V_{approach}$	Last flaps before full + gear	3°	As required to maintain glideslope
[1000, 0]	$V_{approach}$	Full flaps + gear	3°	As required to maintain glideslope
0	[$V_{approach}$, 60]	Full flaps + gear	---	As required for deceleration

Vertical profiles were calculated separately for each representative aircraft type. For each representative aircraft type, a mean profile was calculated by taking the mean altitude of the analysis profiles at 0.1 nautical mile spacing along the ground track. Linear interpolation was used to calculate the altitude of each radar profile at these ground track points. A median profile was then defined as the radar trajectory with the smallest root-mean-squared (RMS) distance from this mean. A plot of all profiles used in the matching analysis grouped by altitude percentile at 5 nautical miles ground track distance from the runway threshold, along with the mean, median, and profile generator matched profiles is shown for the Boeing 737-800 representative type in the left-hand plot of Figure 18. The right-hand plot of Figure 18 shows the altitude, airspeed, thrust, and configuration of the generated profile shown in the left-hand side of the figure. Similar summaries of the

matching analysis and corresponding altitude, airspeed, thrust, and configuration profiles for all representative aircraft types are included in Appendix B.

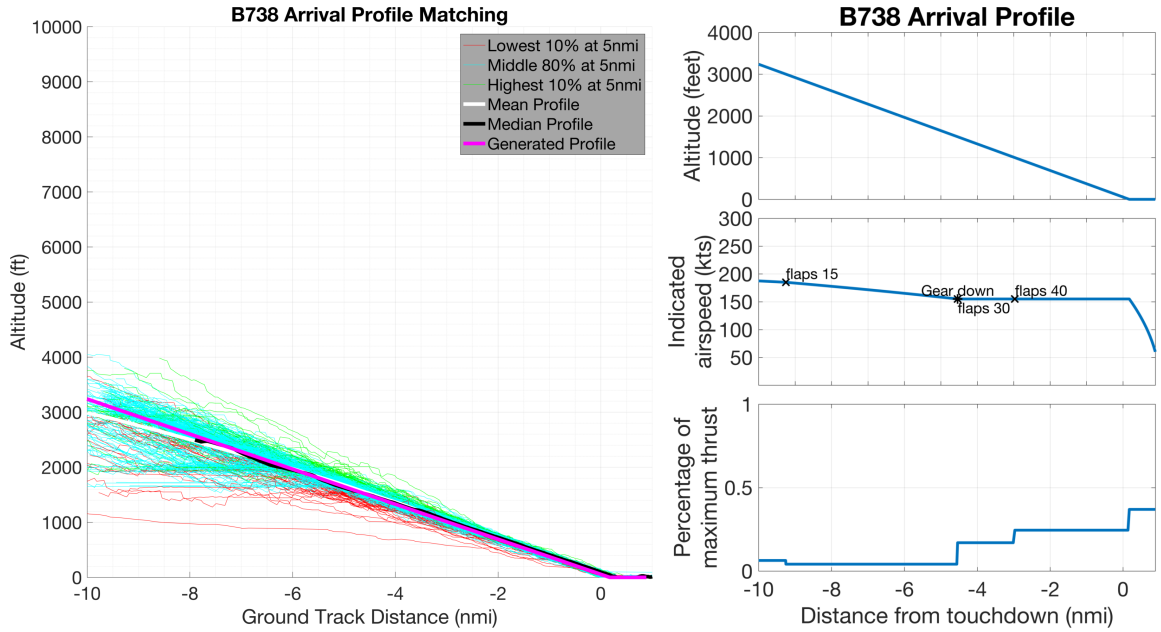

Figure 18: Arrival Profile Altitudes and Matched Arrival Profile for the Boeing 737-800

4.3.2.2 Departures

For departure, procedures exist to determine climb schedules, but specific climb profiles may vary more by aircraft type. The clustered altitude profiles for Boeing 737-800 (B738) departures used for the departure profile matching described in the following paragraphs are shown in Figure 19.

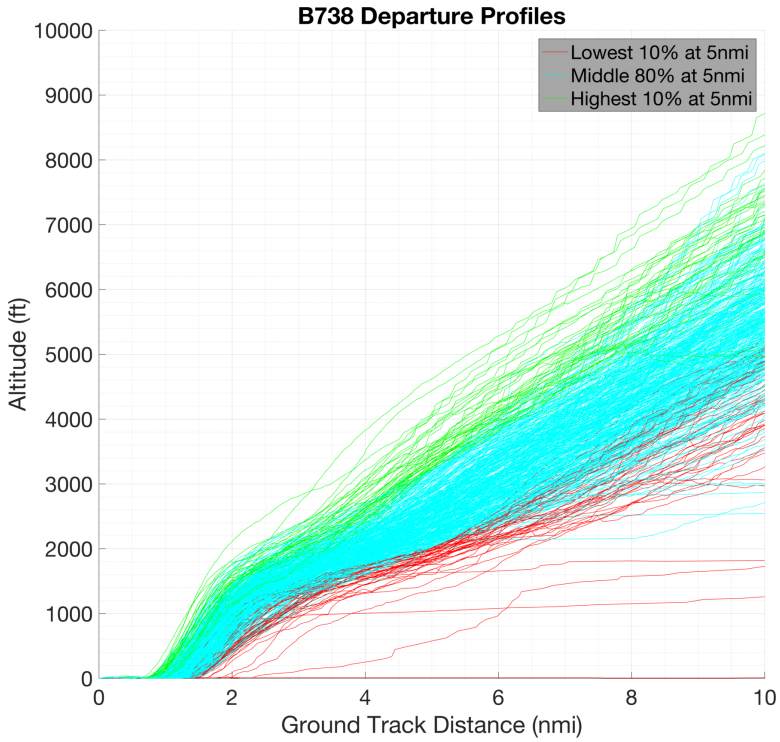

Figure 19: Departure Profile Altitudes from 20 days of ASDE-X data for the Boeing 737-800

For the rapid modeling toolset used for the analysis in this thesis, departures are modeled as flying a modified version of the International Civil Aviation Organization (ICAO) Procedure B departure profile [23] [24]. However, the ICAO B noise abatement procedure does not inherently account for the fact that aircraft often takeoff or climb at a thrust level lower than the maximum for which it is rated for that phase of flight, called de-rated thrust, or that pilots often do a thrust cutback earlier than specified in the ICAO B departure definition. In looking at a selection of ASDE-X data, the 1000' altitude for the beginning of the first acceleration segment, from V_2 to V_2+15knots, did not appear to match well. For these reasons, representative profiles for departure are based on the ICAO B departure procedure but include some changes from the baseline procedure. The final departure definition is shown in Figure 20 and Table 17.

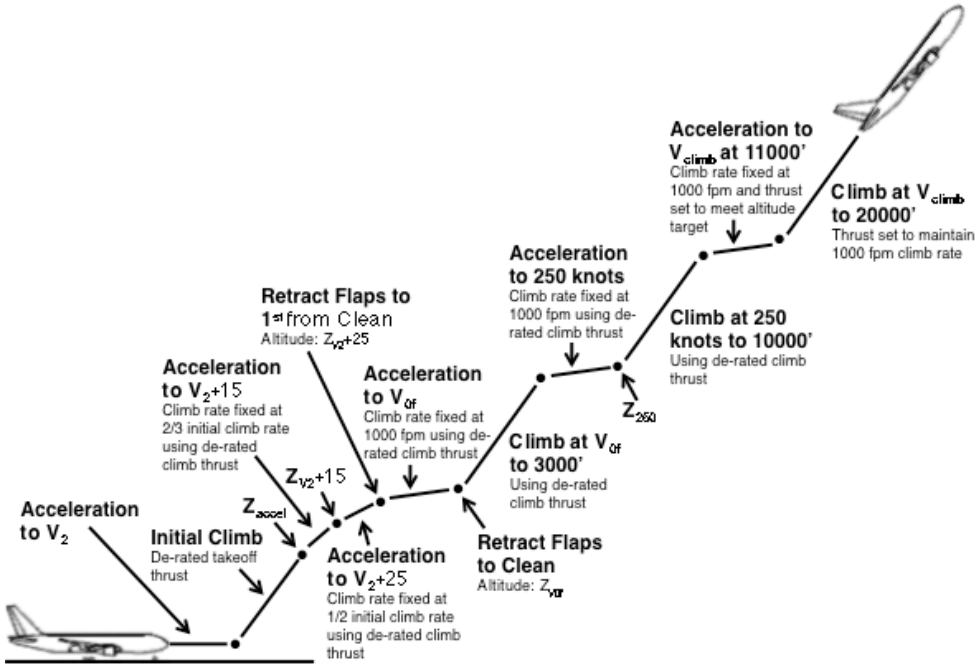

Figure 20: Graphical Depiction of Departure Profile Definition

Table 17: Departure Profile Definition. Adapted and Updated from [23]

Altitude (ft)	Speed (kts IAS)	Configuration	Climb Rate	Thrust
0	[0, V_2]	2nd flaps from clean + gear	---	As required to match takeoff roll
[0, Z_{accel}]	V_2	2nd flaps from clean	Set by thrust (CR_1)	De-rated TO
[Z_{accel}, Z_{V2+15}]	[V_2, V_2+15]	2nd flaps from clean	2/3* CR_1	De-rated Climb
[Z_{V2+15}, Z_{V2+25}]	[V_2+15, V_2+25]	2nd flaps from clean	1/2* CR_1	De-rated Climb
[Z_{V2+25}, Z_{V0f}]	[V_2+25, V_{0f}]	1st flaps from clean	1000 fpm	De-rated Climb
[Z_{V0f}, 3000]	V_{0f}	Clean	Set by thrust	De-rated Climb
[3000, Z_{250}]	[V_{0f}, 250]	Clean	1000 fpm	De-rated Climb
[Z_{250}, 10000]	250	Clean	Set by thrust	De-rated Climb
[10000, 110000]	[250 V_{climb}]	Clean	1000 fpm	As required to maintain climb rate and accelerate in 1000' altitude
[11000, 20000]	V_{climb}	Clean	1000 fpm	As required to maintain climb rate

In this profile, each segment is one of the following: acceleration on the runway to takeoff speed (segment 1), climb at a specified thrust level and constant speed (segment 2, 6, 8, and 10), or acceleration to a set speed during a climb at a fixed climb rate and thrust level (segments 3-5, 7, and 9). For the second segment, Z_{accel} refers to the altitude at which the aircraft begins its first airborne acceleration segment and is set to match the altitude of this initial acceleration seen in radar data. For segments 3-8, the unspecified altitudes are the altitudes at which the target speed for that segment end point is attained (e.g. Z_{250} refers to the altitude at which the aircraft reaches a speed of 250 knots using a fixed climb rate and thrust level). De-rated takeoff and climb thrust are set to match the climb profiles seen in radar data.

Vertical profiles for departure were calculated separately for each representative aircraft type. For each representative aircraft type, mean and median profiles were defined as they were for arrivals: a mean profile was calculated by taking the mean altitude of the analysis profiles at 0.1 nautical mile spacing along the ground track and linear interpolation was used to calculate the altitude of each radar profile at these ground track points. The median profile was then defined as the radar trajectory with the smallest root-mean-squared (RMS) distance from this mean. For departures, however, all matching including for ground roll distance was done to the median profile rather than to a median of values from multiple profiles. Additionally, departures are assumed to begin takeoff roll stopped at the runway threshold (ground track distance and velocity of 0).

For the departure analysis, any profiles with an altitude less than 500’ after 4 nmi from the start of takeoff roll were excluded as the altitude data for these flights was likely inaccurate. Of the remaining data set, all profiles for a given aircraft type with the same runway assignment as the representative lateral trajectory for its parent cluster were included. A plot of all profiles used in the matching analysis grouped by altitude percentile at 5 nautical miles ground track distance from the runway threshold, along with the mean, median, and profile generator matched profiles is shown for the Boeing 737-800 representative type in the left-hand plot of Figure 21. The right-hand plot of Figure 21 shows the altitude, airspeed, thrust, and configuration of the generated profile shown in the left-hand side of the figure. Similar summaries of the matching analysis and

corresponding altitude, airspeed, thrust, and configuration profiles for all representative aircraft types are included in Appendix B.

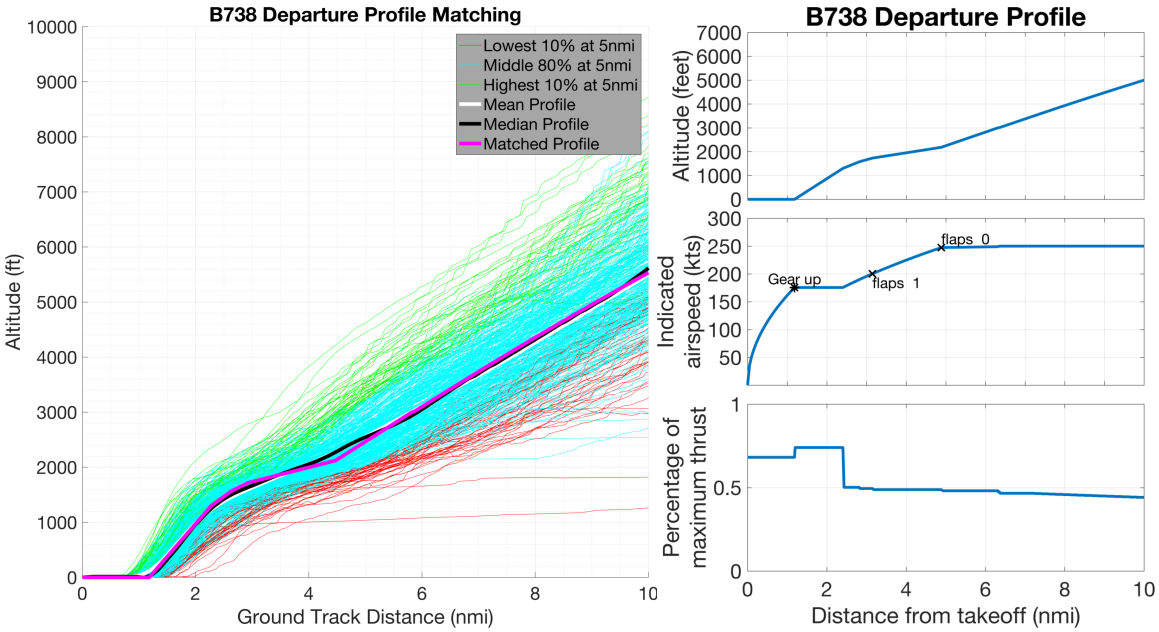

Figure 21: Departure Profile Altitudes and Matched Departure Profile for the Boeing 737-800

4.4 Calculation of Single Flight Noise Results

Given the trajectory and aircraft type information provided by the representative type binning, lateral track analysis, and vertical profile definition, sufficient information exists to calculate noise on a single flight basis. Using a Matlab-AEDT interface developed as part of the rapid aviation environmental impacts modeling effort,[15] SEL and DNL noise results were calculated for each combination of representative lateral track and representative aircraft type with its associated vertical profile using AEDT 2c Service Pack 2 [25].[16]

[15] The majority of the development for this interface was done by Callen Brooks.
[16] Some of these noise results were generated in AEDT by Callen Brooks.

Page Intentionally Left Blank

Chapter 5 Comparison of Annual Average Daily Operations DNL Contours

In order to evaluate the noise modeling approach, this chapter presents a comparison of the annual average DNL calculated using the methodology presented in Chapter 4 against official DNL contours for BOS in 2015 from the annual Environmental Data Report (EDR) published by Massport [3]. Separate maps are shown of each result in Figure 22. It should be noted that these are not on identical scales, although some landmass landmarks can be seen for a rough sizing comparison. A figure of both results overlaid on top of each other is shown in Figure 23. The maps do not line up exactly, likely due to the use of different cartographic projections or coordinate systems, but the figure shows a reasonable approximation of overlaid contours for qualitative comparison purposes. For both Figure 22 and Figure 23, contours are shown at 60, 65, 70, and 75 dB DNL, with the outermost contours being the quietest.

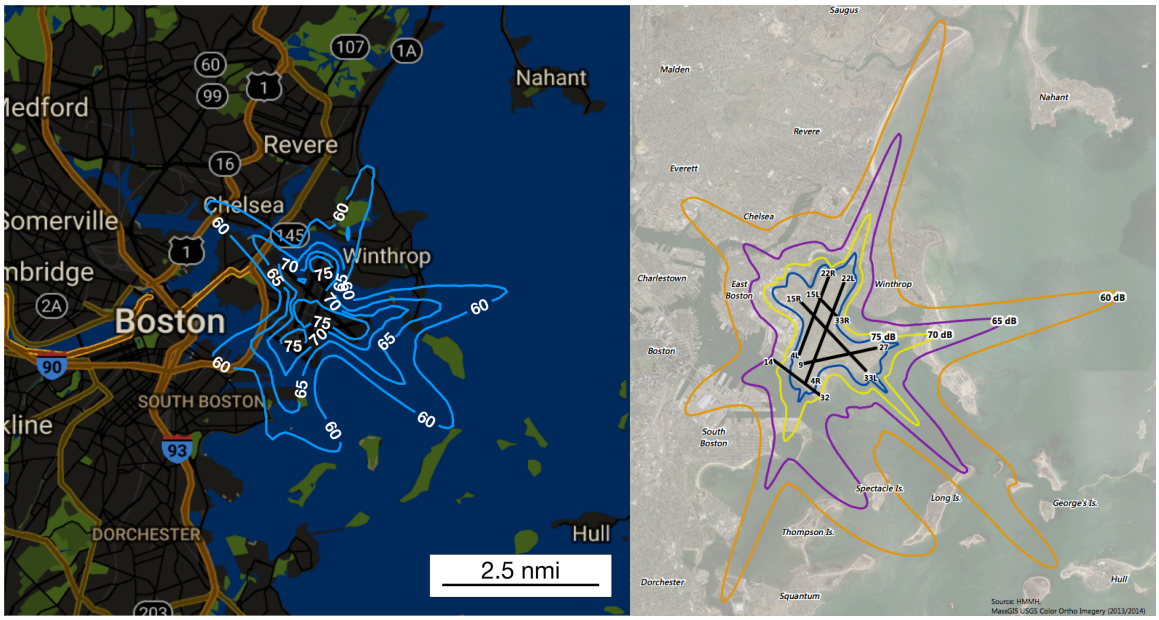

Figure 22: Modeled Annual Average DNL Contours (left) and 2015 BOS Environmental Data Report DNL Contours (right). Source for right-hand image: Massport [3]

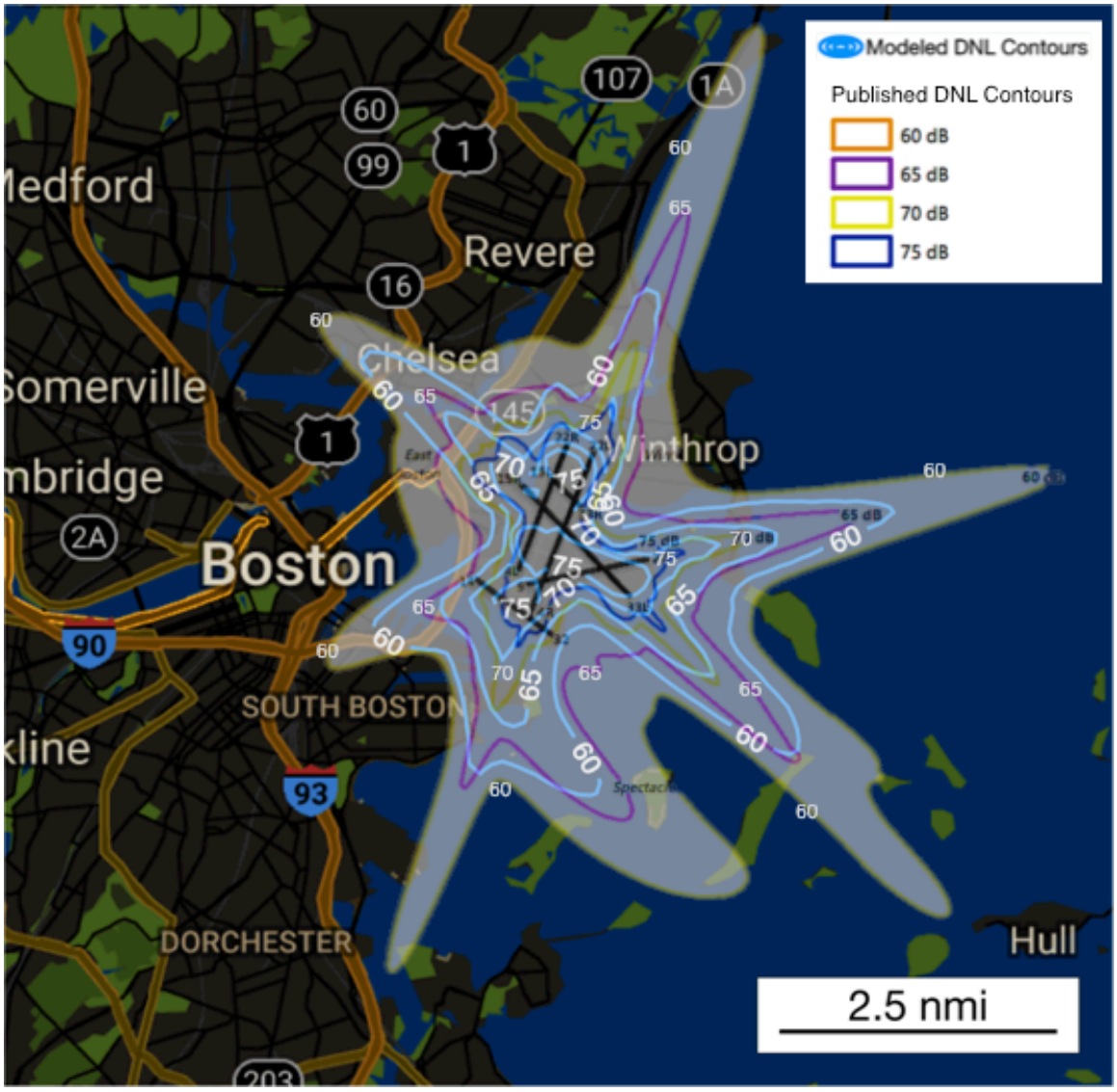

Figure 23: 2015 BOS Environmental Data Report DNL Contours Overlaid on Modeled Annual Average DNL Contours. Note: maps do not have perfect alignment. Source for overlay: Massport [3]

At the 60dB level – the full extent of the shaded area and the outermost light blue contour – the modeled contours are smaller than the corresponding EDR contours. The extent of the contours is fairly similar at a roughly 5-10dB DNL offset, which can be seen by the fact that the outermost light blue contour (60dB modeled) is in many areas close to the purple contour (65dB EDR).

Some possible explanations for these differences lie in modifications made to the noise model itself for the EDR results. The modeling for this thesis was done using the

standard AEDT assumptions, which are those implemented in the only version publically available. In contrast, the modeling for the EDR contours was done using a version of the Integrated Noise Model (INM), the predecessor to AEDT, with modifications specifically for regulatory analysis at BOS. The modifications include an adjustment for the reflectivity of the water around BOS and for a hill just north of the airport [3].[17] Given that these corrections apply only to the water (where there are no complainants) and a small area immediately north of the airport (where there are few complainants), however, it is expected that these corrections would have only a small impact on the results in this analysis.

[17] Additional details about the BOS-specific adjustments used in calculating the EDR contours can be found in [3].

Page Intentionally Left Blank

Chapter 6 Case Study Results

This chapter presents the results of the analysis for the case studies outlined in Chapter 3 using the methodology presented in Chapter 4. Section 6.1 examines the impact of varying the DNL threshold on complainant capture rates for the annual average day scenario. Section 6.2 examines the impacts of changing the representative day scenario on complainant capture rates for DNL. Section 6.3 compares complainant capture rates for DNL and two representative N_{above} $L_{A,max}$ thresholds for the most representative day scenario. A full set of contour maps for all scenarios examined for DNL and N_{above} 55dB, 60dB, 65dB, and 70dB, along with tables showing the contour area, population exposure, and percent of complainants contained for each of these contours, can be found in Appendix C - Appendix E.

6.1 Varying DNL Threshold

This section presents DNL contours for the annual average day scenario and compares complainant capture at the 65dB and lower DNL threshold levels. These DNL contours are shown in Figure 24, overlaid on complainant locations. This figure shows that a very low portion of complainants (<1%) is captured at the 65dB contour level. The 45dB DNL contour, the outermost contour, captures a much larger portion of complainants (57%), but it can be seen that this still fails to capture a substantial number of complainants in the northwest map quadrant (33L departure complainants). Table 18 lists the complainant capture rates for each of these contours.

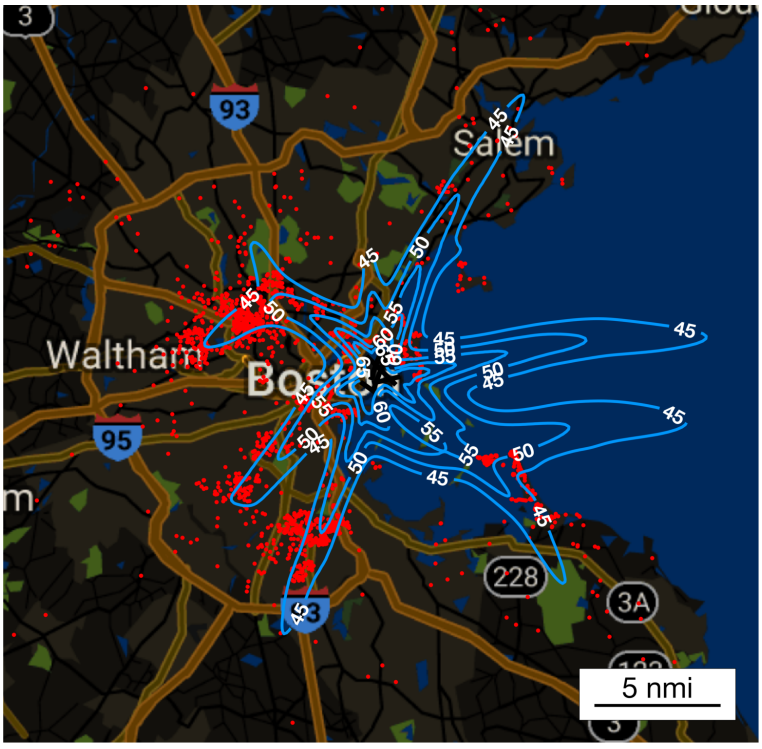

Figure 24: Annual Average Day DNL Contours

Table 18: Annual Average Day Complainant Coverage by DNL Contour Level

Contour Level	% Addresses Contained All Complainants	% Addresses Contained 33L Departure Complainants Only
45dB DNL		
50dB DNL	18.58%	14.66%
55dB DNL	7.31%	8.05%
60dB DNL	3.40%	3.49%
65dB DNL	0.76%	0.12%

6.2 DNL for Varied Representative Day Scenarios

Even at very low levels of 45dB, average annual day DNL does not appear to effectively capture a substantial portion of noise complainants. Since an annual average day represents an average of operations over the course of the year, the concentration is diffused in a particular area and it does not appear to capture complaints associated with specific runway use issues. One approach considered here is to analyze the DNL for a day which represents a high use of a single runway (in this case 33L for departures) to

see if this more accurately captures the noise complaints in the northwest quadrant associated with 33L departures. An even more focused approach is also considered where the flight pattern associated with the hour of most intense use of 33L (33L peak hour) is assumed to have occurred over the entire 24-hour period.

This section examines the impact of changing the representative day scenario examined by analyzing a day of heavy use of a particular departure runway, runway 33L, and by also looking at the impact of the heaviest hour of departures, if that hour of operations were flown for a full 24 hours. Since these specific day and hour scenarios will impact only certain areas of complainants, the results in this section will show the relative effectiveness of DNL in capturing complainants in the northwest map quadrant only (33L departure complainants).

Figure 25, Figure 26, and Figure 27 show DNL 45-65dB contours for all three representative day scenarios – the annual average day, the 33L peak day, and the 33L peak hour. These figures show that the annual average misses coverage of a large fraction of complainants (only capturing 54%) at the 45dB DNL level. At this same DNL threshold, the 33L peak day and 33L peak hour scenarios do capture a substantial fraction of complainants (87% and 93% respectively). However, the 33L peak day contours capture these complainants with substantially less overreach in terms of contour extent beyond complainant areas than the 33L peak hour scenario. For the 33L peak day scenario, it appears that effective complainant capture begins somewhere within the 45-50dB DNL threshold range.

The complainant containment numbers for each DNL contour examined are shown in Table 19. In this table, all contours that capture less than 30% of complainants are shaded red for poor complainant capture, all contours that capture 30%-70% of complainants are shaded yellow for moderate complainant capture, and all contours that capture more than 70% of complainants are shaded green for substantial complainant capture. Table 20 shows the corresponding contour areas and population exposures for each contour, with the same coloring applied to each contour as in Table 19.

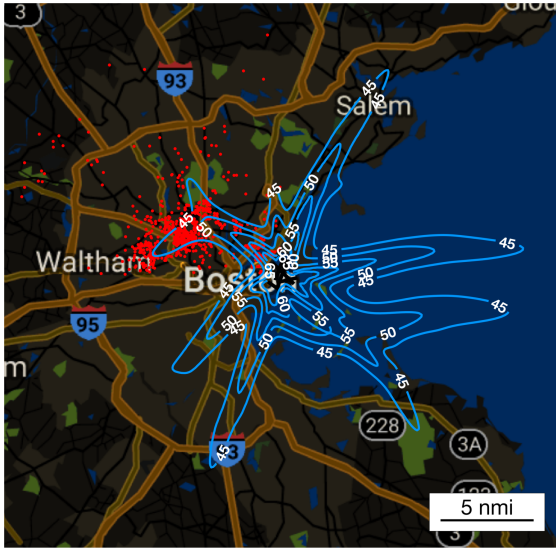

Figure 25: Annual Average Day DNL Contours

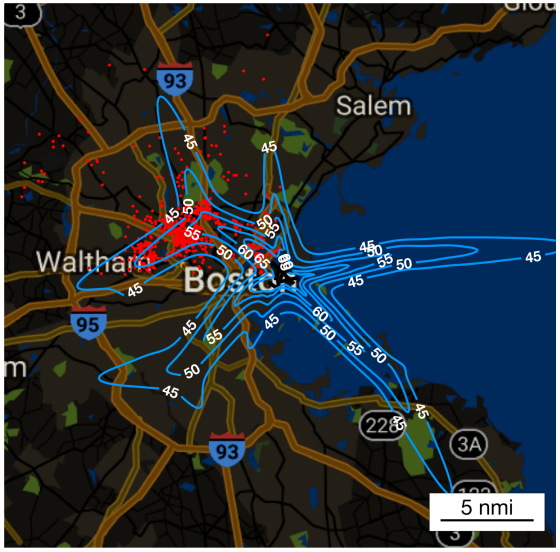

Figure 26: 33L Peak Day DNL Contours

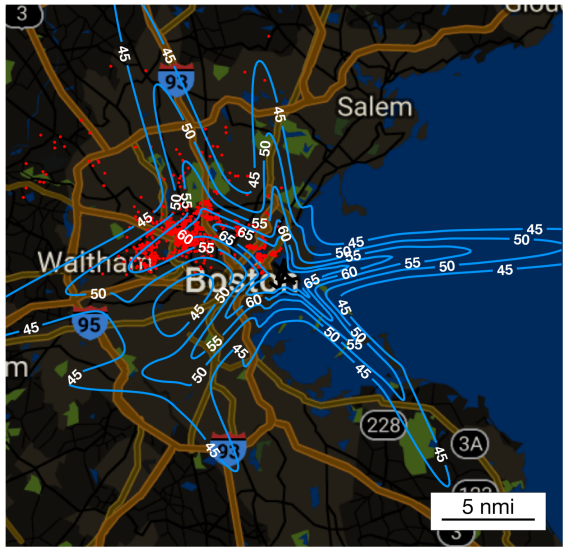

Figure 27: 33L Peak Hour DNL Contours

Table 19: 33L Departures Complainant Coverage for All Scenarios by DNL Contour Level

Contour Level	Annual Average Day	33L Peak Day	33L Peak Hour
45dB DNL	54.21%	87.26%	93.39%
50dB DNL	14.66%	66.11%	88.94%
55dB DNL	8.05%	21.27%	74.04%
60dB DNL	3.49%	8.53%	30.05%
65dB DNL	0.12%	5.17%	9.38%

Table 20: Contour Area and Population Exposure for All Scenarios by DNL Contour Level

Contour Level	Annual Average Day		33L Peak Day		33L Peak Hour	
	Contour Area (nmi^2)	Pop Exposure	Contour Area (nmi^2)	Pop Exposure	Contour Area (nmi^2)	Pop Exposure
45dB DNL	107.43	554,679	114.80	879,087	236.90	1,345,823
50dB DNL	47.88	198,862	51.54	443,925	98.30	795,659
55dB DNL	20.28	61,017	21.86	153,988	43.44	384,738
60dB DNL	7.99	19,852	9.18	49,200	18.24	131,671
65dB DNL	3.38	1,568	3.76	17,640	7.94	50,955

These numeric results confirm the qualitative assessment of complainant capture from the contour maps. The 33L peak hour 50dB DNL contour captures a similar fraction of complainants (89%) to the 45dB DNL 33L peak day contour (87%). These contours also have generally similar population exposure (~800k-875k) and contour area (~100-115nmi^2) indicating similar precision in terms of complainant capture between the 45dB DNL contour for the 33L peak day scenario and the 50dB contour for the 33L peak hour scenario.

Since the 33L peak day scenario is simpler to understand and to analyze compared to the 33L peak hour scenario, a representative single day of operations is more desirable for use as an alternative to annual average day analysis. In addition, assuming peak traffic for 24 hours is not realistic and overrepresents the noise impact. The results of this analysis show that for the case of heavy use of 33L, examining a representative day of a single configuration at the 45dB DNL level is sufficient to capture a significant fraction of complainants.

6.3 Evaluation of N_{above}

An additional approach to capturing overflight noise concerns is the use of N_{above} metrics. These metrics are somewhat more complicated than DNL, as they include both noise level and overflight count thresholds making the matrix of possible thresholds to evaluate two-dimensional.

This section evaluates N_{above} for the 33L peak day scenario using two different noise thresholds (60dB day/50dB night and 65dB day/55dB night) and a series of overflight count contours for each and compares the complainant coverage of these contours with DNL complainant coverage. These thresholds for N_{above} analysis were selected for discussion based on a preliminary analysis of thresholds from 55dB day/45dB night – 70dB day/60dB night, which showed substantial overreach of contours beyond complainant areas at the 55dB threshold and very weak complainant coverage at the 70dB level. Results for all four thresholds examined for the 33L peak day can be found in Appendix D. It is important to note that this section only presents analysis for a configuration using 33L departures and that examination of other configurations might yield different results or insights.

Figure 28 shows the DNL contours, Figure 29 shows the N_{above} 60dB day contours, and Figure 30 shows the N_{above} 65dB day contours for the 33L peak day scenario. The DNL shows substantial overshoot of complainant areas at the 45dB level, particularly near the Waltham marker and the northern I-93 marker. The N_{above} 60dB day/50dB night shows coverage of a substantial fraction of complainants at the 25 and 50 overflight contour levels with fairly low overshoot of many of the complainant areas. The N_{above} 65dB day/55dB night shows relatively poor complainant coverage for all of the contours examined. This implies that 65dB is too high a noise threshold for a N_{above} metric to effectively capture more than a moderate fraction of complainants for the 33L peak day scenario.

Table 21 shows the complainant capture rates for all N_{above} 60dB and 65dB day overflight contours, shaded in the same manner as Table 19 and Table 20 in Section 6.2. Table 22 shows the corresponding contour areas and population exposures for each contour, with the same coloring applied to each contour as in Table 21.

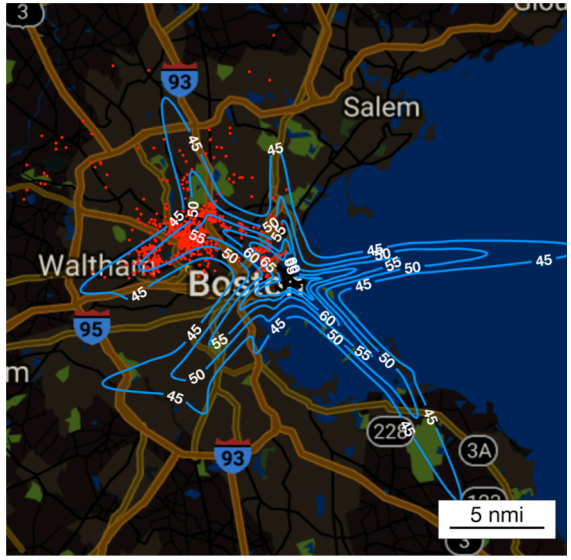

Figure 28: 33L Peak Day DNL Contours

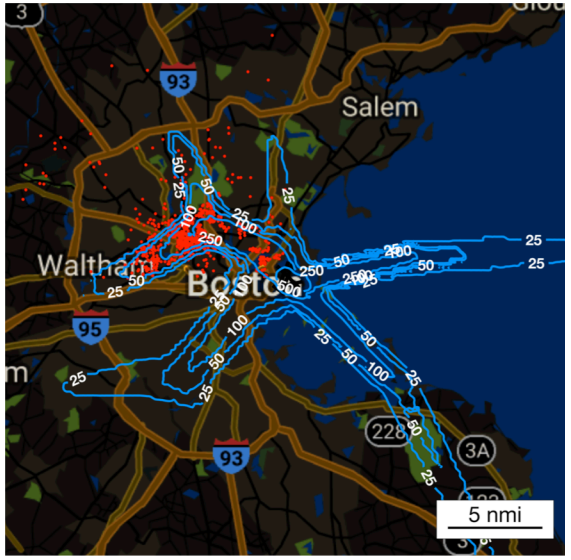

Figure 29: 33L Peak Day N_{above} 60dB Day/50dB Night Contours

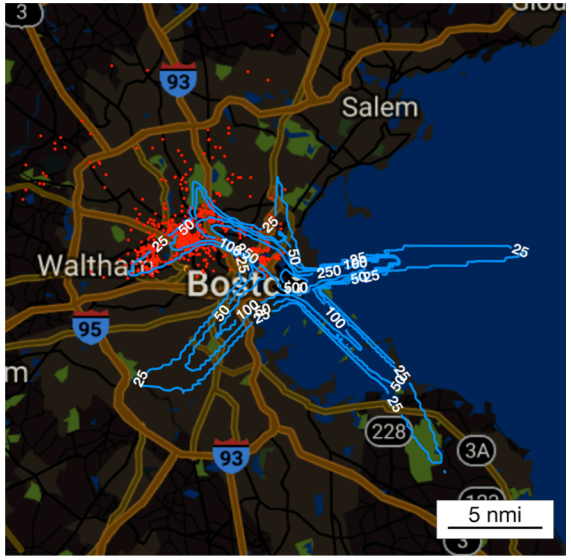

Figure 30: 33L Peak Day N_{above} 65dB Day/55dB Night Contours

Table 21: 33L Departures Complainant Coverage for 33L Peak Day Scenario by Contour Level, N_{above} 60dB Day/50dB Night and N_{above} 65dB Day/55dB Night

Contour Level	N_{above} 60dB day, 50dB night	N_{above} 65dB day, 55dB night
25 flights	84.25%	67.07%
50 flights	77.52%	47.60%
100 flights	55.53%	16.95%
250 flights	20.31%	9.74%
500 flights	0.00%	0.00%

Table 22: Contour Area and Population Exposure for 33L Peak Day Scenario by Contour Level, N_{above} 60dB Day/50dB Night and N_{above} 65dB Day/55dB Night

Contour Level	N_{above} 60dB day, 50dB night		N_{above} 65dB day, 55dB night	
	Contour Area (nmi^2)	Pop Exposure	Contour Area (nmi^2)	Pop Exposure
25 flights	123.35	850,795	63.64	505,246
50 flights	63.50	539,846	32.94	261,543
100 flights	35.93	263,884	16.88	92,988
250 flights	13.26	82,796	6.83	46,686
500 flights	1.73	0	1.03	0

These results indicate that for N_{above} 60dB day/50dB night, the 25 and 50 overflight contours capture a similar number of complainants (84% and 78%, respectively) compared to the 45dB DNL contour (87%). The 25 overflight contour has a similar area and population exposure to the 45dB DNL contour (Table 20) and captures a similar number of complainants. The 50 overflight contour more precisely captures a substantial fraction of complainants – although it covers a smaller number of complainants than the 25 overflight and the 45dB DNL contours it still captures the along-track extent of a large number of complainants. This indicates that N_{above} 60dB day at an average of 25-50 overflights per day (1-2 flights per hour) captures annoyance similarly to DNL levels of 45dB and 50dB, but that neither N_{above} nor DNL is necessarily a more effective metric for capturing annoyance due to aviation noise exposure given the scenarios analyzed.

Chapter 7 Conclusion

The goals of the analysis in this thesis were to compare the extent to which the use of different operational scenarios and the extent to which using N_{above} noise metrics as opposed to DNL thresholds below 65dB change the effectiveness with which noise contours capture locations of high annoyance. Three case studies at BOS were examined as part of this comparison – one looking at all complainants in the context of a representative annual average day, one looking at complainants related specifically to usage of runway 33L for departures in the context of a day of heavy usage of that runway, and one looking at the same set of complainants in the context of the 33L peak hour of departures during that day.

The first set of results presented in this thesis showed greater 33L complainant coverage at a given noise threshold for the 33L peak day compared to an annual average day. They showed coverage of a substantial fraction of complainants (66%-87%) at the 45dB-50dB DNL thresholds for the 33L peak day scenario. The results showed that the 33L peak hour analysis captured a similar fraction of complainants to the 33L peak day analysis, but without substantially different contour shapes or sizes. Since a representative day of operations is easier to understand conceptually and to analyze, that scenario is likely preferable for use in future analysis. These results imply that future noise impact analysis should independently examine individual runway configurations, rather than analyzing noise impacts on an annual average basis, to effectively capture annoyance. Results should be examined down to the 45dB DNL level to have a reasonable likelihood of capturing a significant portion of annoyance.

The second set of results, regarding the effectiveness of DNL vs. N_{above}, indicated that examining DNL at a threshold level of roughly 45dB captured a similar proportion of complainants to N_{above} 60dB day/50dB night at the 25-50 overflight level for the 33L peak day scenario. There did not appear to be a strong benefit in terms of complainant coverage to using either metric as long as appropriate thresholds were used for analysis for each.

It is important to note that the results presented here examine only one specific airport and one specific runway configuration with a high number of departures from runway 33L at BOS. These results are not necessarily portable to other runway configurations at BOS or to analysis at other airports since specific configurations may generate different exposure patterns. So further analysis examining other runway configurations at BOS or annoyance patterns at other airports will likely be valuable in further understanding the limitations and generalizability of the conclusions of this thesis. The systematic analysis conducted in this thesis demonstrates one method by which these future studies might be conducted.

Appendix A Representative Aircraft Bin Assignment

ICAO Type Code	Bin
2TH	SRJ
A124	TA
A306	OJ
A310	OJ
A318	A320
A319	A320
A320	A320
A321	A320
A332	TA
A333	TA
A340	TA
A342	TA
A343	TA
A345	TA
A346	TA
AC11	PNJ
AC50	PNJ
AC69	PNJ
AC90	SRJ
AC95	SRJ
AEST	PNJ
ASTR	SRJ
B190	SRJ
B350	SRJ
B712	OJ
B717	OJ
B722	OJ
B733	B737
B734	B737
B735	B737
B737	B737
B738	B737
B739	B737
B744	TA
B747	TA
B748	TA

ICAO Type Code	Bin
B74S	TA
B752	B757
B753	B757
B757	B757
B762	TA
B763	TA
B764	TA
B767	TA
B772	TA
B777	TA
B77L	TA
B77W	TA
B787	TA
B788	TA
B789	TA
BE10	SRJ
BE20	SRJ
BE24	PNJ
BE30	SRJ
BE33	PNJ
BE35	PNJ
BE36	PNJ
BE40	SRJ
BE55	PNJ
BE56	PNJ
BE58	PNJ
BE76	PNJ
BE90	SRJ
BE95	PNJ
BE9L	SRJ
BE9T	SRJ
C150	PNJ
C152	PNJ
C172	PNJ
C177	PNJ
C180	PNJ

ICAO Type Code	Bin
C182	PNJ
C206	PNJ
C208	SRJ
C210	PNJ
C25A	SRJ
C25B	SRJ
C25C	SRJ
C310	PNJ
C340	PNJ
C402	PNJ
C414	PNJ
C421	PNJ
C441	SRJ
C500	SRJ
C501	SRJ
C510	SRJ
C525	SRJ
C550	SRJ
C560	SRJ
C56X	SRJ
C650	SRJ
C680	SRJ
C72R	PNJ
C750	SRJ
C82R	PNJ
CL30	SRJ
CL60	SRJ
CL65	SRJ
CN35	SRJ
COL3	PNJ
COL4	PNJ
CRJ	SRJ
CRJ2	SRJ
CRJ7	LRJ
CRJ9	LRJ
D328	SRJ
DA40	PNJ
DA42	PNJ

ICAO Type Code	Bin
DA50	PNJ
DA7X	SRJ
DC10	OJ
DC93	OJ
DEFI	PNJ
DH8	PNJ
DH8A	SRJ
DH8C	SRJ
DH8D	SRJ
E135	SRJ
E145	SRJ
E170	LRJ
E190	LRJ
E45X	SRJ
E50P	SRJ
E550	SRJ
E55P	SRJ
EA50	SRJ
EVOT	SRJ
F900	SRJ
FA10	SRJ
FA20	SRJ
FA50	SRJ
FA7X	SRJ
FALC	PNJ
FBA2	PNJ
G150	SRJ
G280	SRJ
GALX	SRJ
GL5T	SRJ
GLEX	SRJ
GLF2	SRJ
GLF3	SRJ
GLF4	SRJ
GLF5	SRJ
GLF6	SRJ
GLST	PNJ
H25B	SRJ

ICAO Type Code	Bin
H25C	SRJ
HA4T	SRJ
J328	SRJ
JS31	SRJ
LJ25	SRJ
LJ31	SRJ
LJ35	SRJ
LJ40	SRJ
LJ45	SRJ
LJ55	SRJ
LJ60	SRJ
LNCE	PNJ
M020	PNJ
M20A	PNJ
M20P	PNJ
M20T	PNJ
M7	PNJ
MAUL	PNJ
MD11	OJ
MD81	OJ
MD82	OJ
MD83	OJ
MD87	OJ
MD88	OJ
MD90	OJ
MO20	PNJ
MU2	SRJ
MU30	SRJ
P28A	PNJ
P28B	PNJ
P28R	PNJ
P28T	PNJ

ICAO Type Code	Bin
P32A	PNJ
P32R	PNJ
P46T	SRJ
PA23	PNJ
PA24	PNJ
PA27	PNJ
PA28	PNJ
PA30	PNJ
PA31	PNJ
PA32	PNJ
PA34	PNJ
PA44	PNJ
PA46	PNJ
PASE	UNK
PAY1	SRJ
PAY2	SRJ
PAZT	UNK
PC12	SRJ
PRM1	SRJ
RV6	PNJ
SBR1	SRJ
SF34	SRJ
SR20	PNJ
SR22	PNJ
SW3	SRJ
TB21	PNJ
TBM7	SRJ
TBM8	SRJ
TRIN	UNK
VTUR	PNJ
WW24	SRJ

Page Intentionally Left Blank

Appendix B Representative Type Profiles

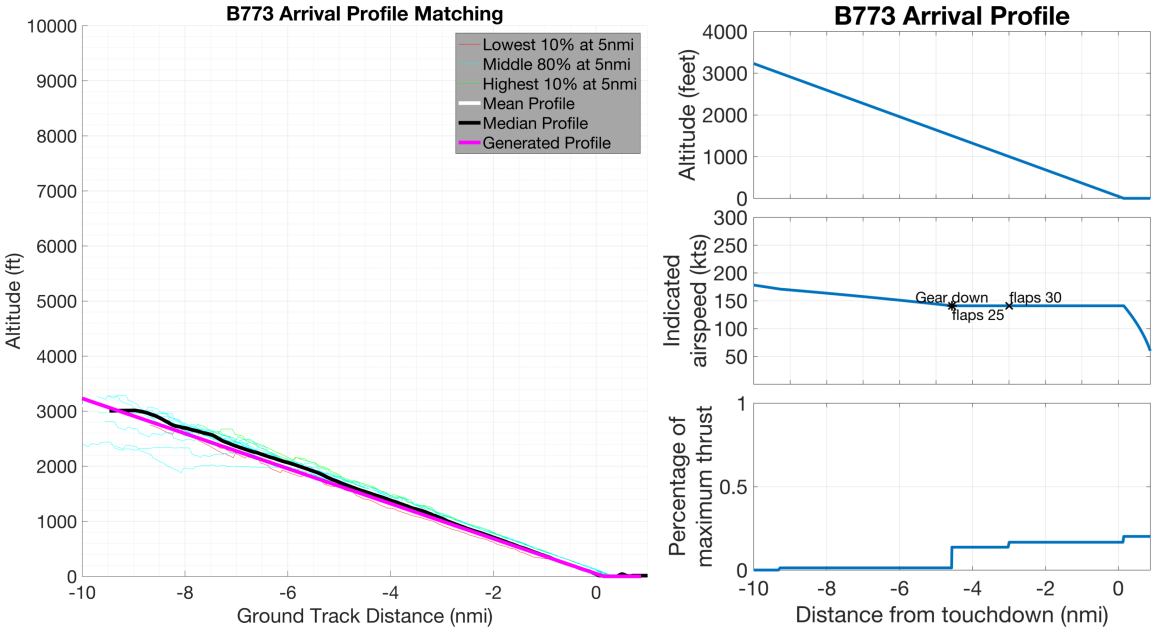

Arrival Profile Altitudes and Matched Arrival Profile for the Boeing 777-300 and 777-300ER[18]

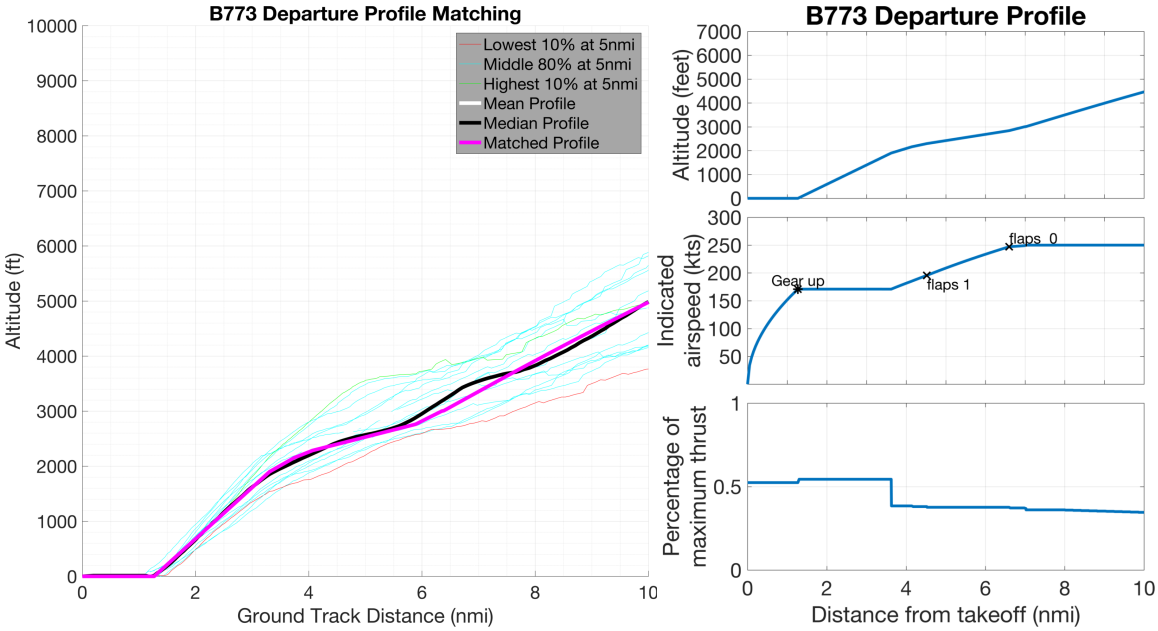

Departure Profile Altitudes and Matched Departure Profile for the Boeing 777-300 and 777-300ER[18]

[18] 777-300ER included in profile analysis due to low volume of Boeing 777-300 flights.

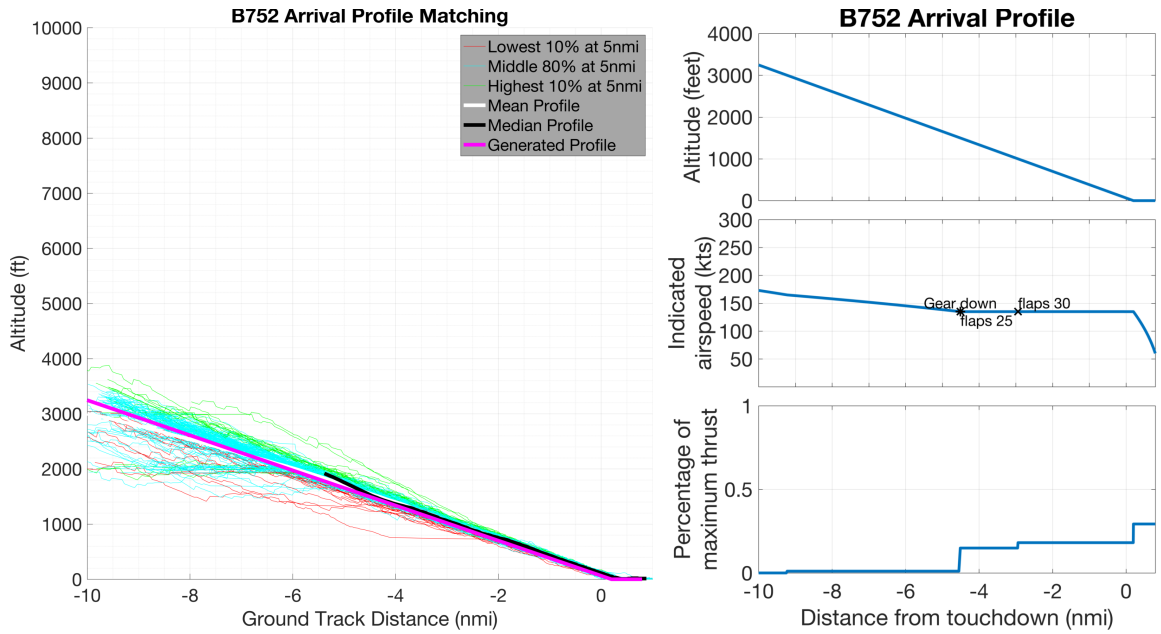

Arrival Profile Altitudes and Matched Arrival Profile for the Boeing 757-200

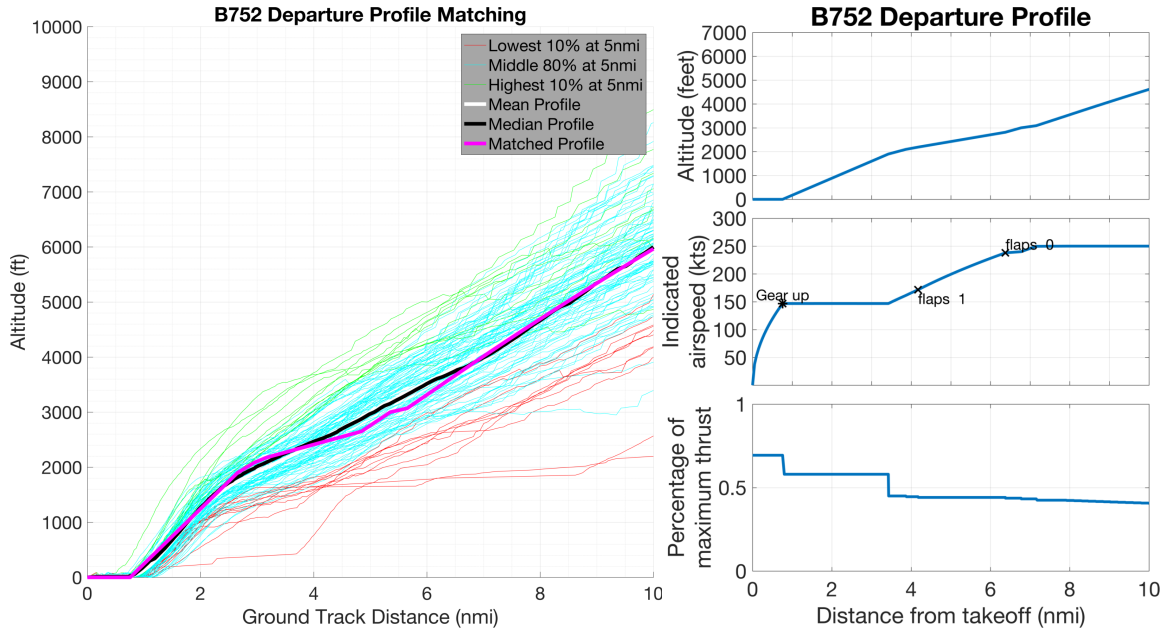

Departure Profile Altitudes and Matched Departure Profile for the Boeing 757-200

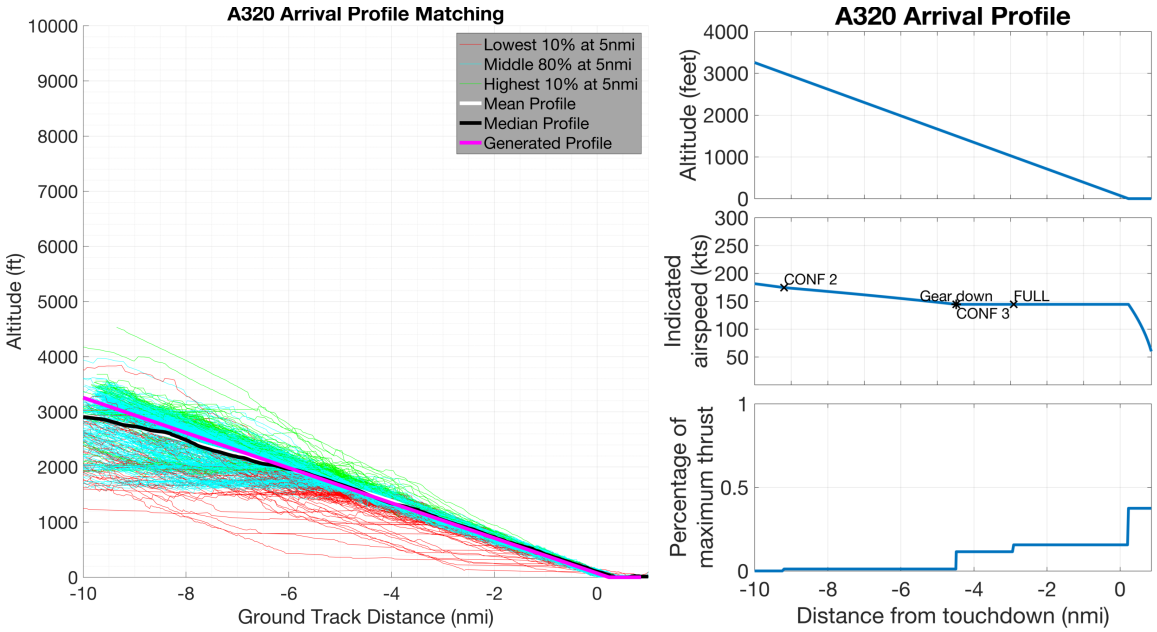

Arrival Profile Altitudes and Matched Arrival Profile for the Airbus A320-212

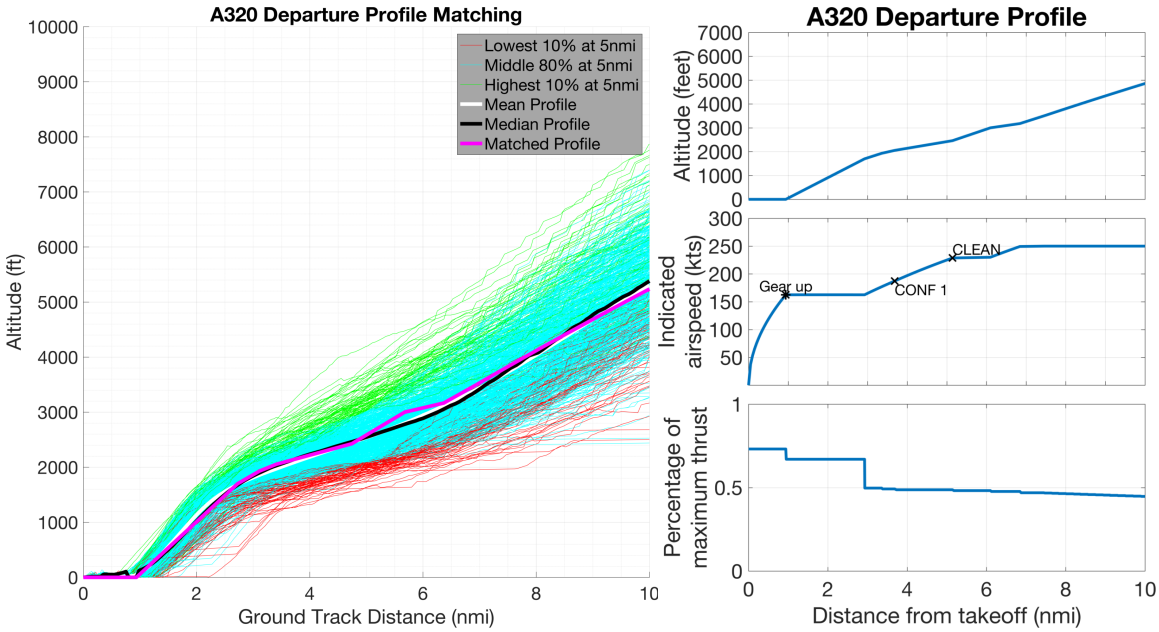

Departure Profile Altitudes and Matched Departure Profile for the Airbus A320-212

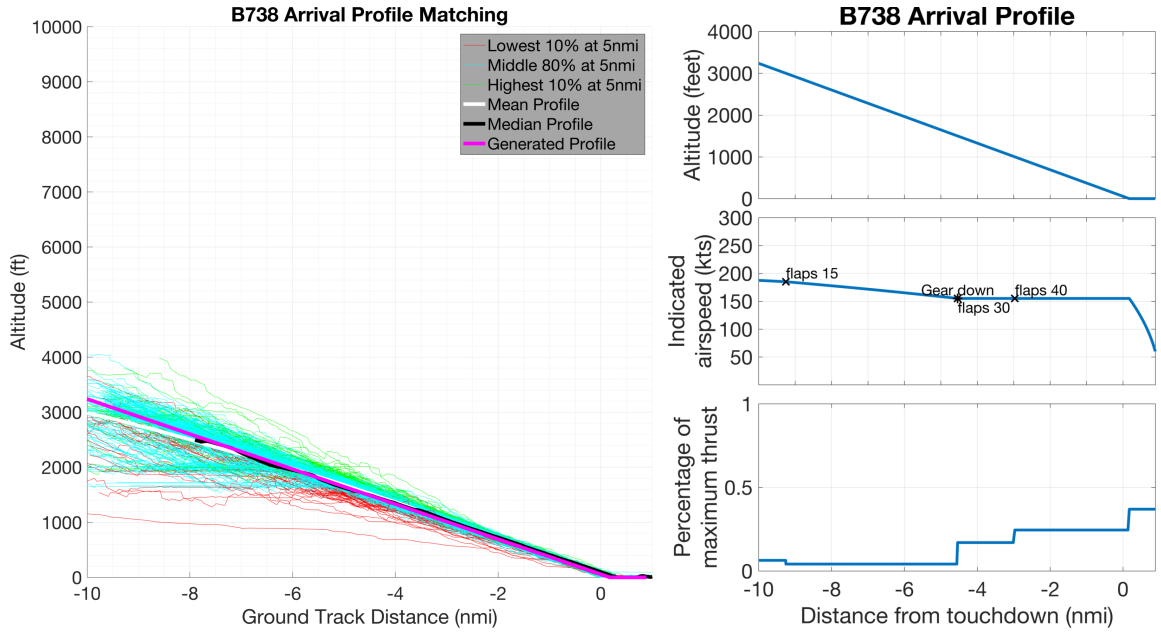

Arrival Profile Altitudes and Matched Arrival Profile for the Boeing 737-800

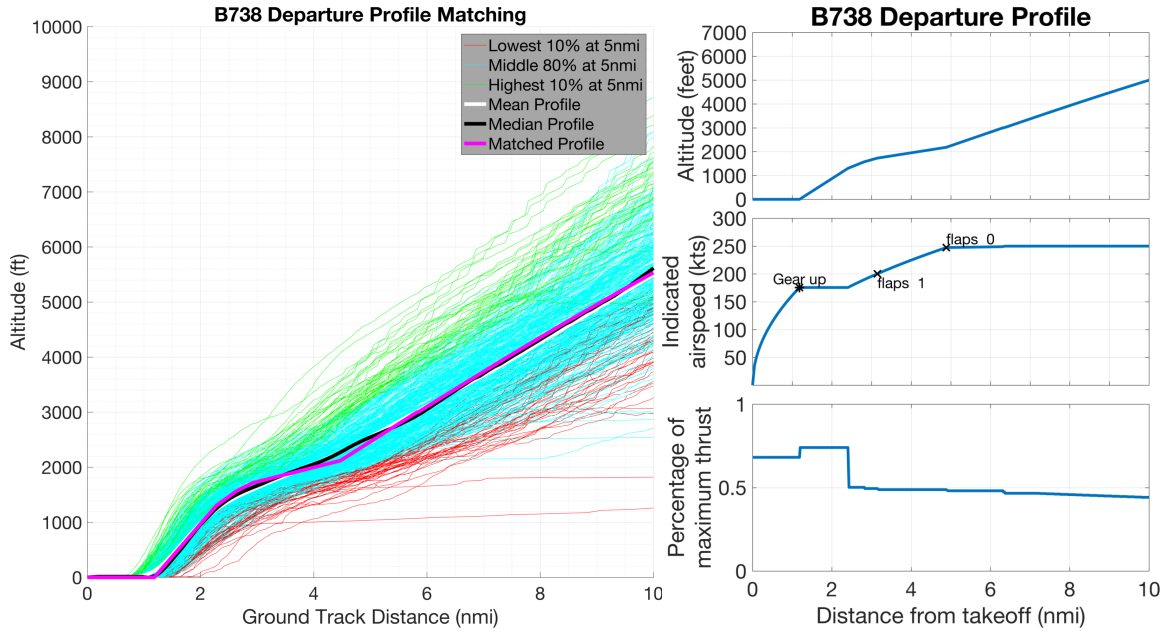

Departure Profile Altitudes and Matched Departure Profile for the Boeing 737-800

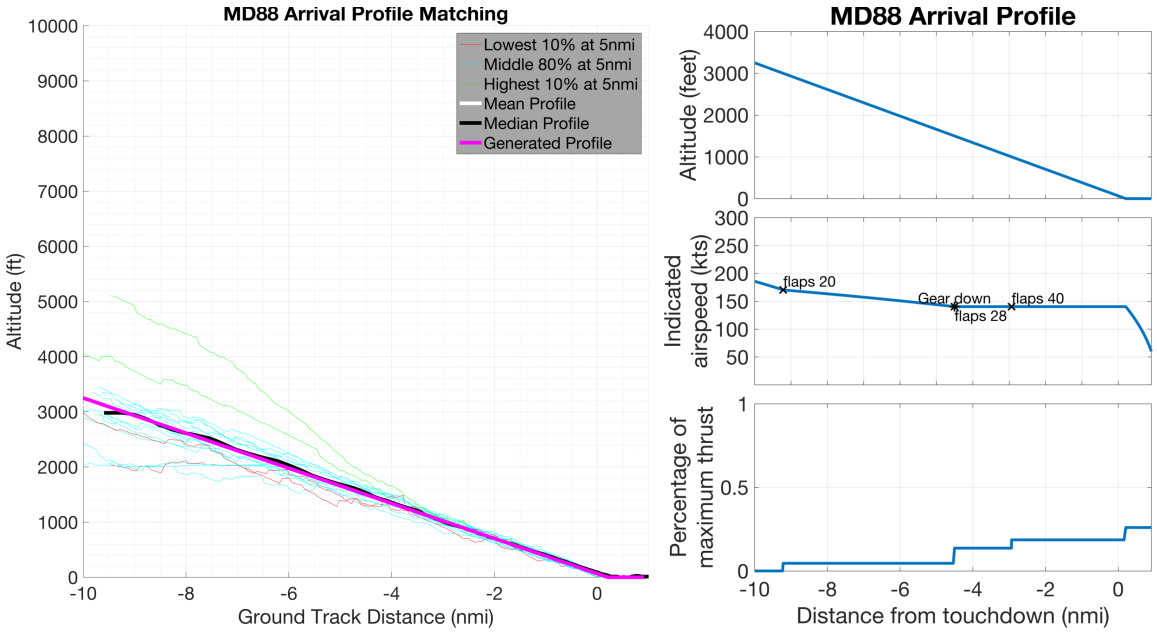

Arrival Profile Altitudes and Matched Arrival Profile for the McDonnell Douglas MD-88

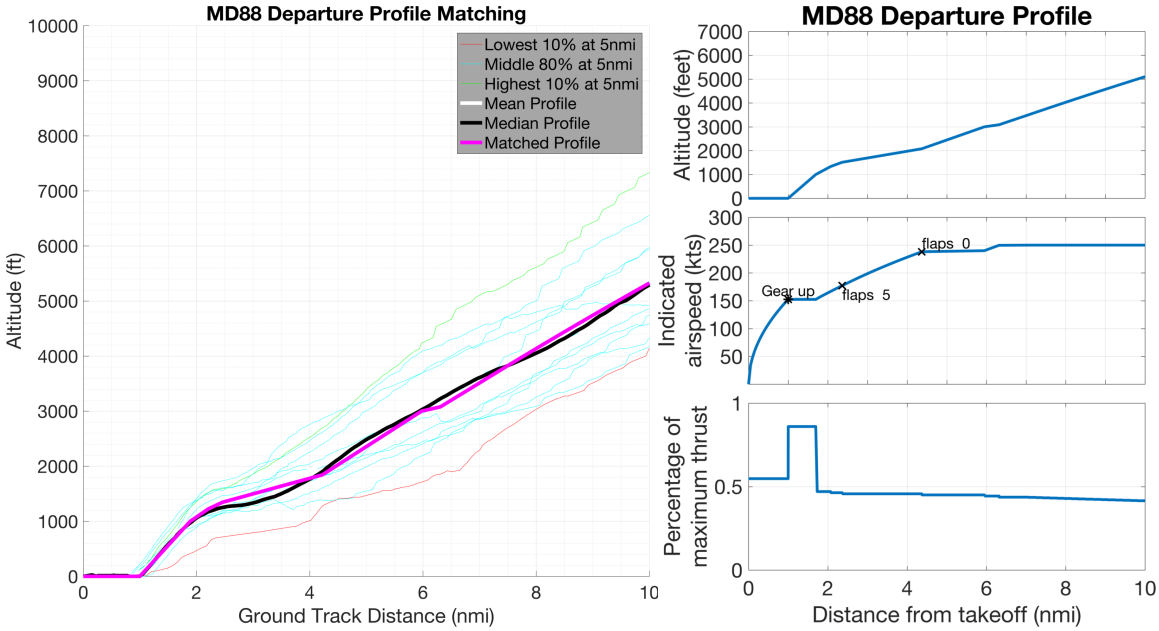

Departure Profile Altitudes and Matched Departure Profile for the McDonnell Douglas MD-88

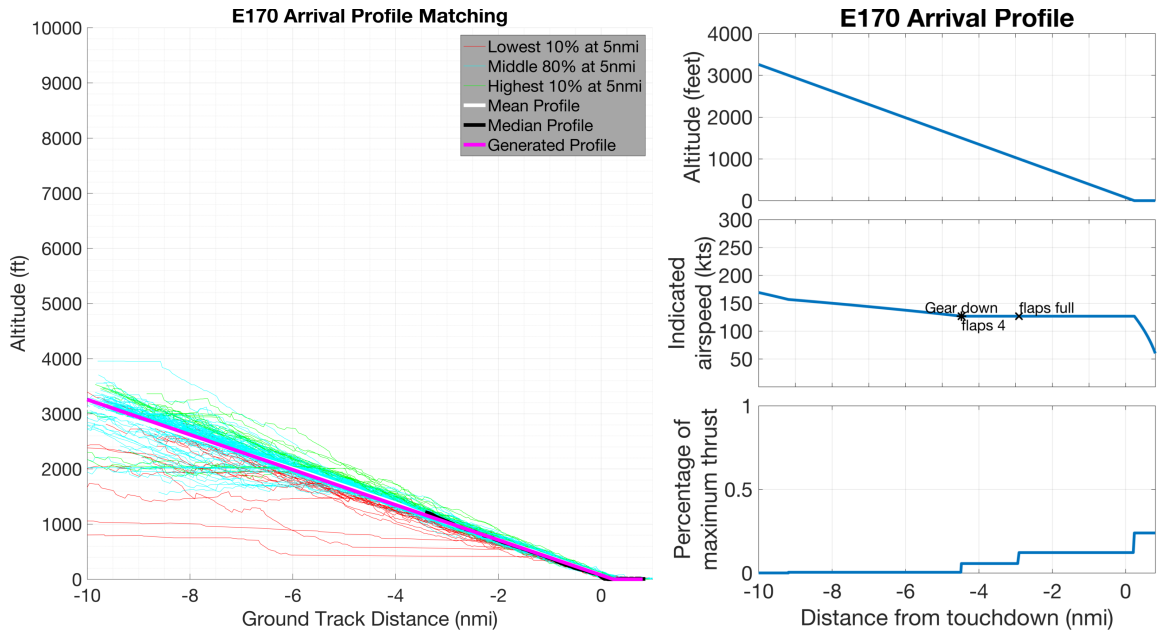

Arrival Profile Altitudes and Matched Arrival Profile for the Embraer E-170LR

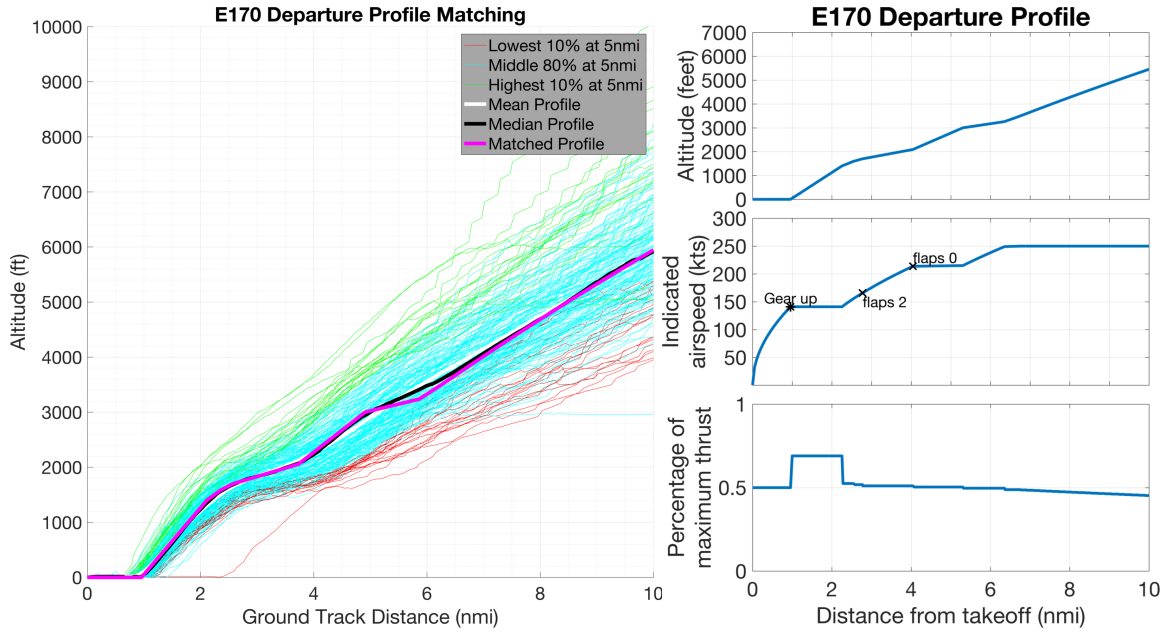

Departure Profile Altitudes and Matched Departure Profile for the Embraer E-170LR

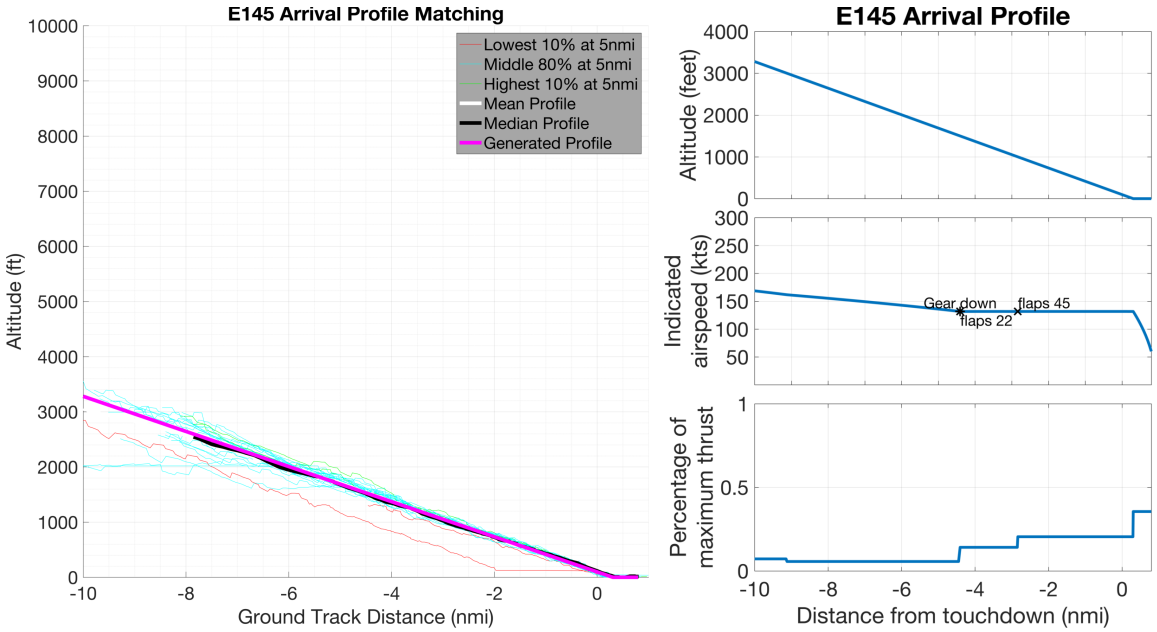

Arrival Profile Altitudes and Matched Arrival Profile for the Embraer E-145LR

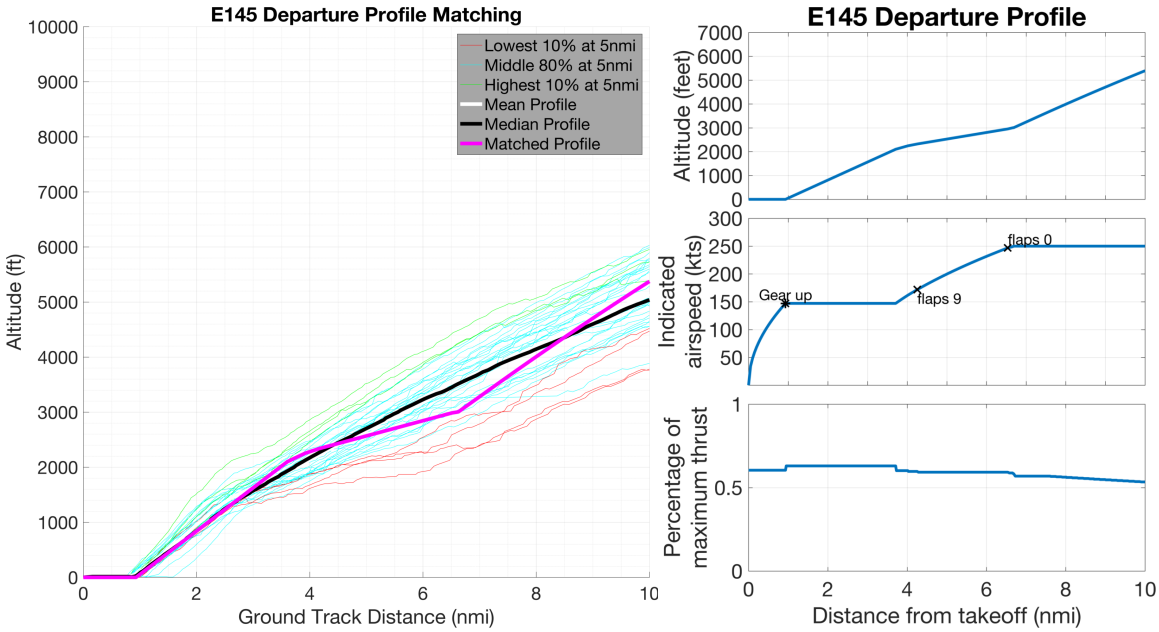

Departure Profile Altitudes and Matched Departure Profile for the Embraer E-145LR

Page Intentionally Left Blank

Appendix C Annual Average Day Analysis Results: Contour Maps and Tables of Contour Area, Population Exposure, and Complainant Coverage by Contour

Metric Comparison Table

Noise Metric	Contour Level	Contour Area (nmi^2)	Population Exposure	% Addresses Contained, All Complainants	% Addresses Contained, 33L Departure Complainants Only
DNL					
	50dB	47.88	198,862	18.58%	14.66%
	55dB	20.28	61,017	7.31%	8.05%
	60dB	7.99	19,852	3.40%	3.49%
	65dB	3.38	1,568	0.76%	0.12%
N_{above} 55dB day, 45dB night	25 flights	201.55	873,575	77.26%	79.33%
	50 flights	110.63	515,458	47.61%	26.56%
	100 flights	56.54	144,946	25.53%	7.21%
	250 flights	8.95	19,382	3.35%	0.84%
	500 flights	1.99	1	0.00%	0.00%
N_{above} 60dB day, 50dB night	25 flights	99.60	499,902	53.86%	51.68%
	50 flights	58.71	245,917	29.24%	16.11%
	100 flights	31.06	53,859	9.75%	3.25%
	250 flights	4.71	4,626	1.68%	0.00%
	500 flights	1.03	0	0.00%	0.00%
N_{above} 65dB day, 55dB night	25 flights	51.19	213,988	18.63%	14.18%
	50 flights	30.63	92,042	10.86%	10.46%
	100 flights	14.38	15,552	3.05%	0.36%
	250 flights	2.89	13	0.05%	0.00%
	500 flights	0.55	0	0.00%	0.00%
N_{above} 70dB day, 60dB night	25 flights	27.44	76,079	8.53%	8.41%
	50 flights	13.90	35,825	5.38%	5.53%
	100 flights	6.19	5,344	1.83%	0.00%
	250 flights	1.61	0	0.00%	0.00%
	500 flights	0.23	0	0.00%	0.00%

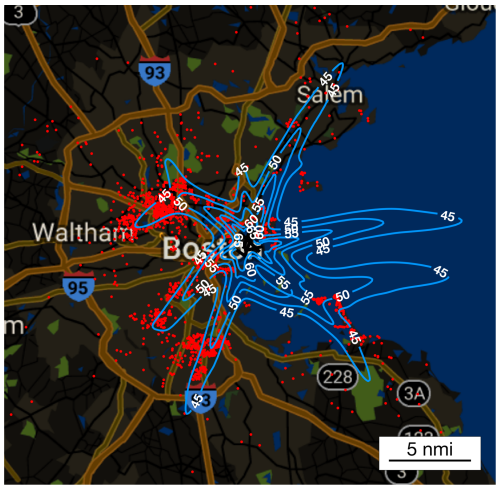

DNL Contours

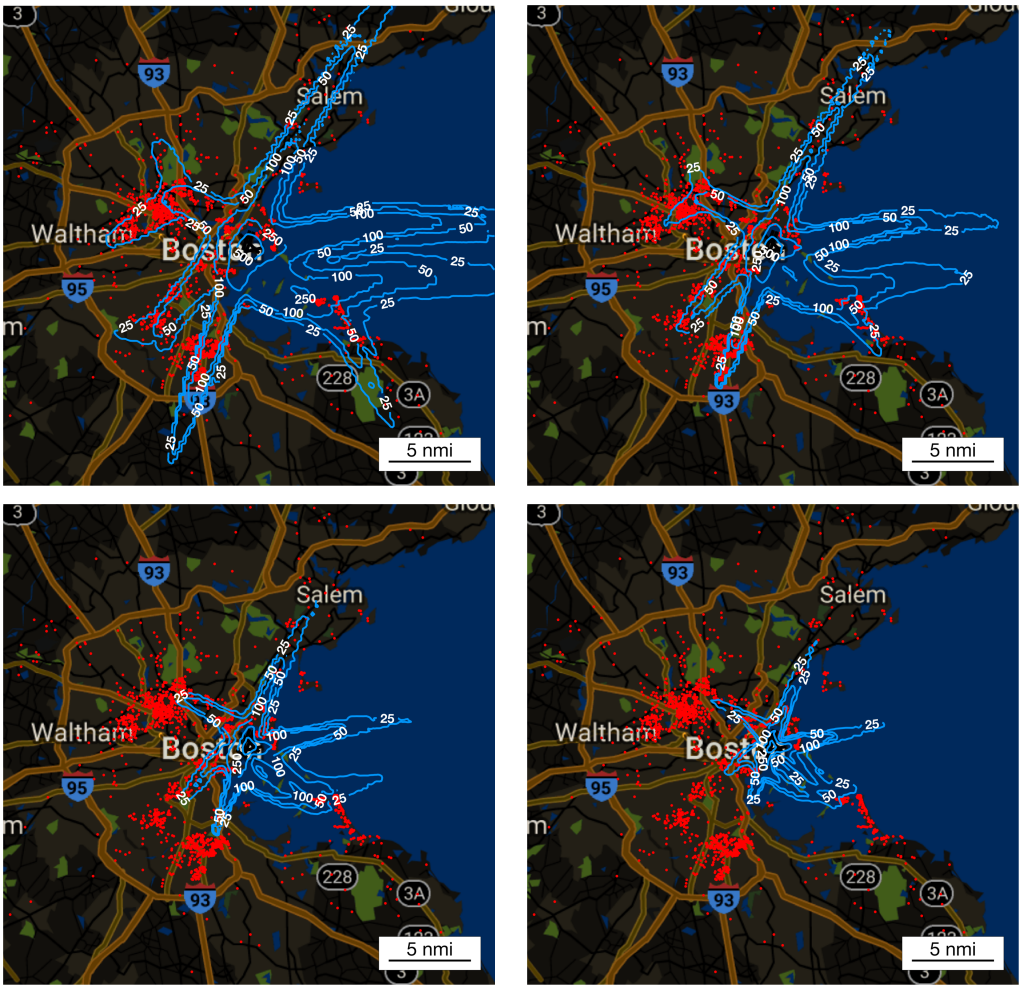

N_{above} Contours: 55dB Day, 45dB Night (upper left); 60dB Day, 50dB Night (upper right); 65dB Day, 55dB Night (lower left); 70dB Day, 60dB Night (lower right)

Appendix D 33L Peak Day Analysis Results: Contour Maps and Tables of Contour Area, Population Exposure, and Complainant Coverage by Contour

Metric Comparison Table

Noise Metric	Contour Level	Contour Area (nmi^2)	Population Exposure	% Addresses Contained, 33L Departure Complainants Only
DNL				
	50dB	51.54	443,925	66.11%
	55dB	21.86		21.27%
	60dB	9.18	49,200	8.53%
	65dB	3.76		5.17%
N_{above} 55dB day, 45dB night	25 flights	263.34	1,230,749	90.14%
	50 flights	125.33		87.74%
	100 flights	69.45	544,591	82.33%
	250 flights	23.96		34.25%
	500 flights	3.11	870	0.00%
N_{above} 60dB day, 50dB night	25 flights	123.35		84.25%
	50 flights	63.50	539,846	77.52%
	100 flights	35.93		55.53%
	250 flights	13.26	82,796	20.31%
	500 flights	1.73		0.00%
N_{above} 65dB day, 55dB night	25 flights	63.64	505,246	67.07%
	50 flights	32.94		47.60%
	100 flights	16.88	92,988	16.95%
	250 flights	6.83		9.74%
	500 flights	1.03	0	0.00%
N_{above} 70dB day, 60dB night	25 flights	32.74		38.94%
	50 flights	16.89	100,029	12.50%
	100 flights	8.51		9.25%
	250 flights	3.21	20,832	6.01%
	500 flights	0.57		0.00%

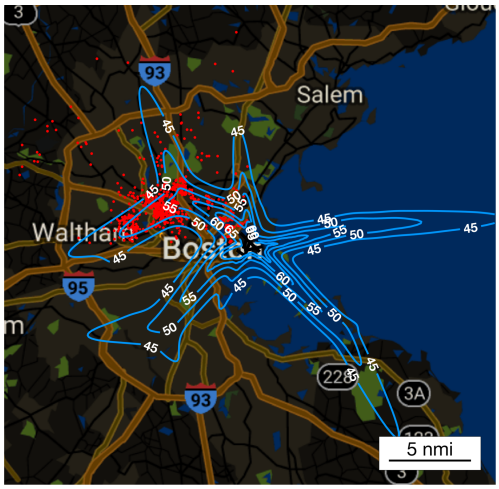

DNL Contours

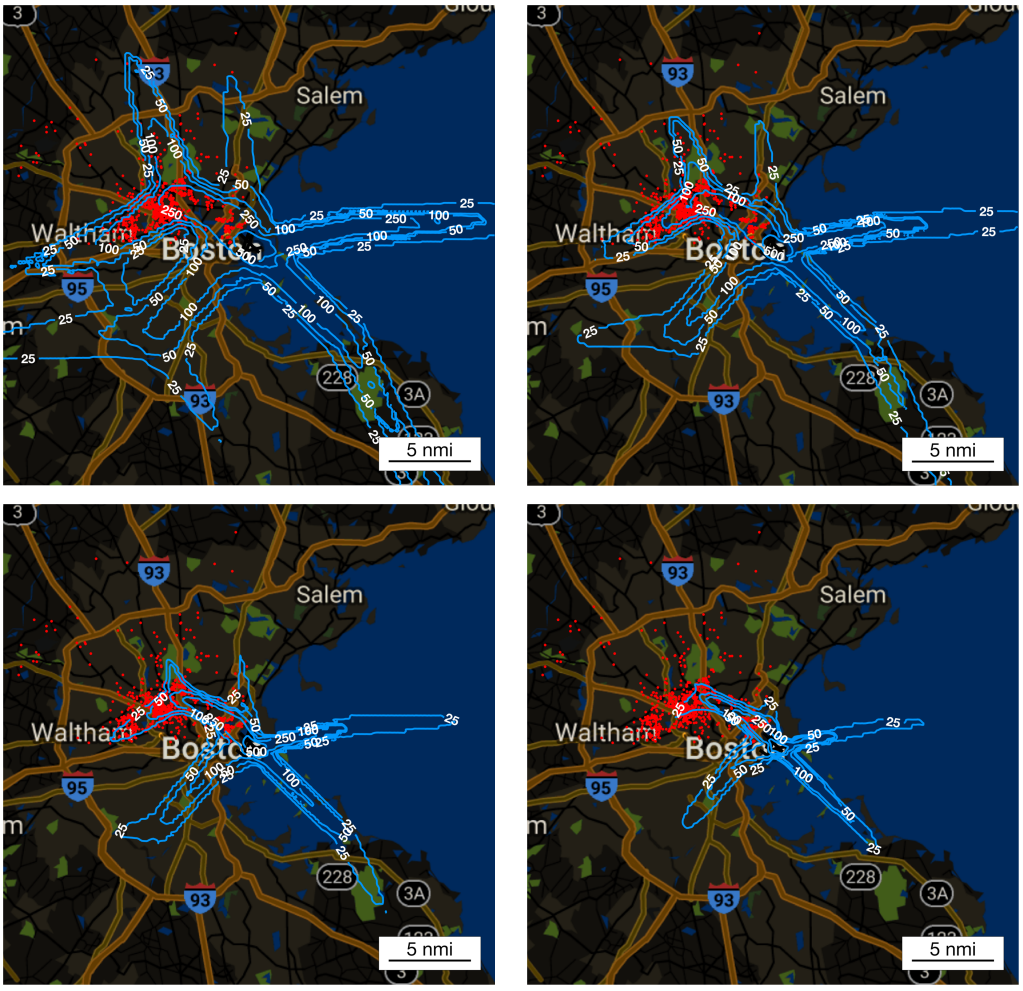

N_{above} Contours: 55dB Day, 45dB Night (upper left); 60dB Day, 50dB Night (upper right); 65dB Day, 55dB Night (lower left); 70dB Day, 60dB Night (lower right)

Appendix E 33L Peak Hour Analysis Results: Contour Maps and Tables of Contour Area, Population Exposure, and Complainant Coverage by Contour

Metric Comparison Table

Noise Metric	Contour Level	Contour Area (nmi^2)	Population Exposure	% Addresses Contained, 33L Departure Complainants Only
DNL				
	50dB	98.30	795,659	88.94%
	55dB	43.44	384,738	74.04%
	60dB	18.24	131,671	30.05%
	65dB	7.94	50,955	9.38%
N_{above} 55dB day, 45dB night	25 flights	463.17	1,813,843	95.43%
	50 flights	305.57	1,471,698	93.99%
	100 flights	187.75	1,066,803	91.11%
	250 flights	58.78	468,932	86.42%
	500 flights	22.19	235,070	61.18%
N_{above} 60dB day, 50dB night	25 flights	231.54	1,279,828	91.59%
	50 flights	136.35	979,783	90.14%
	100 flights	91.24	678,714	87.74%
	250 flights	32.82	295,770	75.36%
	500 flights	13.20	128,415	34.13%
N_{above} 65dB day, 55dB night	25 flights	105.79	833,274	88.34%
	50 flights	69.46	609,588	84.38%
	100 flights	46.06	362,679	78.97%
	250 flights	17.04	159,359	46.03%
	500 flights	7.29	55,359	11.54%
N_{above} 70dB day, 60dB night	25 flights	53.87	480,036	78.37%
	50 flights	37.18	323,599	68.27%
	100 flights	22.67	168,861	49.88%
	250 flights	9.29	66,354	14.78%
	500 flights	3.54	31,019	7.57%

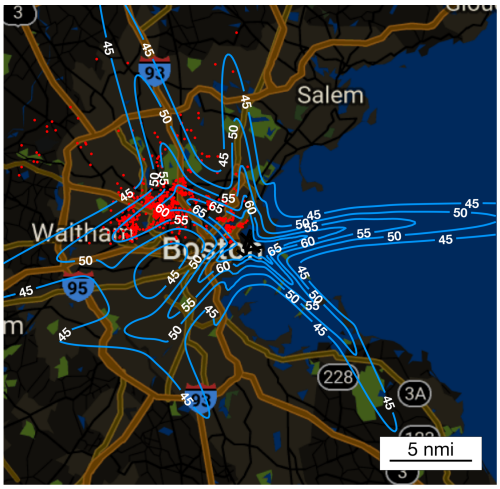

DNL Contours

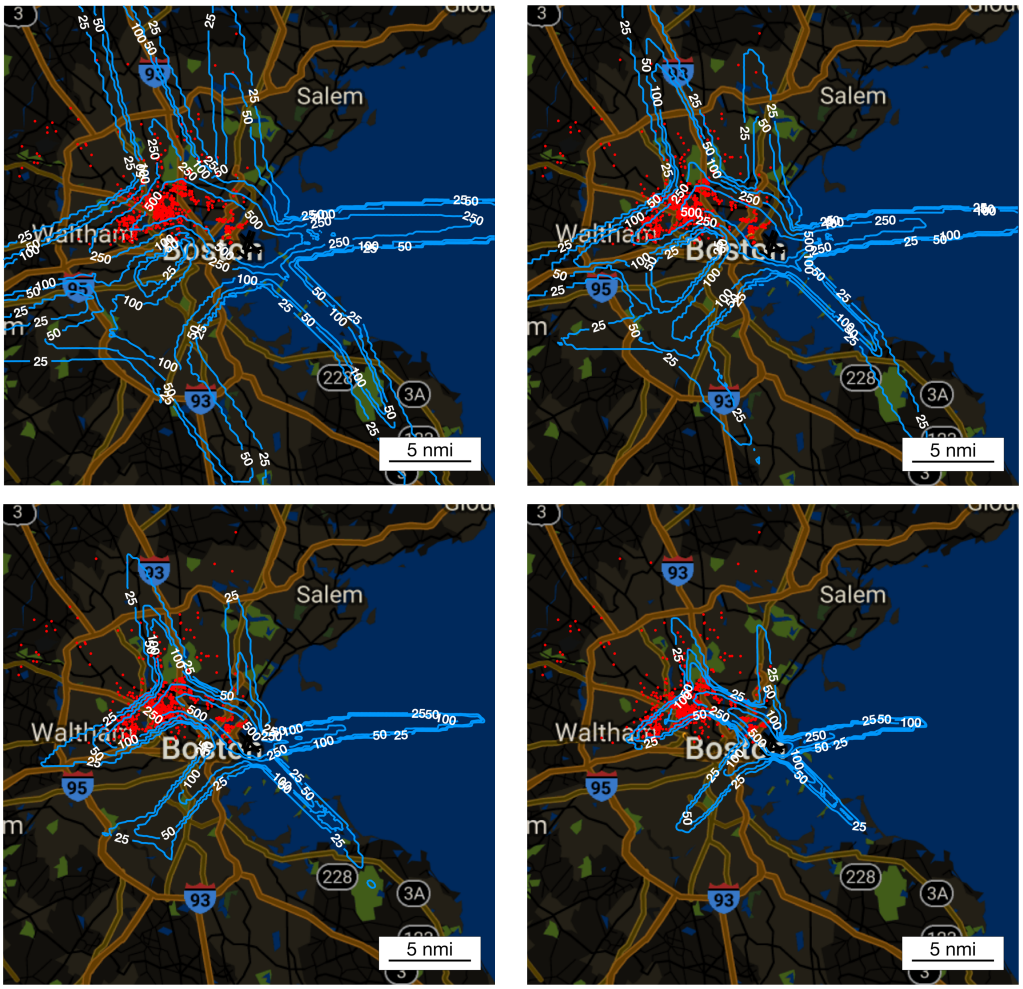

N_{above} Contours: 55dB Day, 45dB Night (upper left); 60dB Day, 50dB Night (upper right); 65dB Day, 55dB Night (lower left); 70dB Day, 60dB Night (lower right)

References

[1] Federal Aviation Administration, "NextGen – Performance Based Navigation," 2017. [Online]. Available: https://www.faa.gov/nextgen/update/progress_and_plans/pbn/. [Accessed: 23-May-2017].

[2] Massport and R. J. Hansman, "Massport and FAA RNAV Pilot Study Overview Public Briefing," 2017. [Online]. Available: https://www.massport.com/media/423551/DRAFT-RNAV-MOU-Meeting-022217-Final2.pdf. [Accessed: 17-May-2017].

[3] Massachusetts Port Authority, "2015 Environmental Data Report," 2016.

[4] M. J. T. Smith, *Aircraft Noise*. Cambridge University Press, 1989.

[5] D. Driscoll, "OSHA Technical Manual (OTM) | Section III: Chapter 5 - Noise | Occupational Safety and Health Administration," *Occupational Safety and Health Administration*, 2006. [Online]. Available: https://www.osha.gov/dts/osta/otm/new_noise/. [Accessed: 09-May-2017].

[6] M. Ahearn *et al.*, "AEDT 2b Technical Manual," 2016.

[7] G. Reindel, "Overview of Noise Metrics and Acoustical Objectives," in *AAAE Sound Insulation Symposium*, 2001.

[8] A. A. Trani and J. Roa, "CEE 4674 Airport Planning and Design: Sample Airport Noise Computations." [Online]. Available: http://128.173.204.63/courses/cee4674/cee4674_pub/BasicNoiseCalculations.pdf. [Accessed: 09-May-2017].

[9] Boston West Fair Skies, "About Us." [Online]. Available: https://www.bostonwestfairskies.org/attorneys.html. [Accessed: 22-May-2017].

[10] Federal Aviation Administration, "The FAR Part 150 Airport Noise Compatibility Planning Program: An Overview." [Online]. Available: https://www.faa.gov/about/office_org/headquarters_offices/apl/noise_emissions/planning_toolkit/media/II.B.pdf. [Accessed: 14-May-2017].

[11] "eCFR — Code of Federal Regulations." [Online]. Available: https://www.ecfr.gov/cgi-bin/text-idx?SID=8ee55dcc630ed62cc0c85b23a749d508&mc=true&node=pt14.3.150&rgn=div5. [Accessed: 15-May-2017].

[12] M. E. Eagan, "The History of DNL 65 and Implications for Future Noise Policy," in *FAA New England Region 2010 Airports Conference*, 2010.

[13] I. Ricondo & Associates, "Boston Logan Airport Noise Study Final Report," 2017.

[14] T. J. Schultz, "Synthesis of social surveys on noise annoyance," *J. Acousitcal Soc. Am.*, vol. 64, no. 2, pp. 377–405, 1978.

[15] N. P. Miller *et al.*, "Research Methods for Understanding Aircraft Noise Annoyances and Sleep Disturbance," 2014.

[16] Massport, "How Logan Operates: Airfield Layout and Runway Operations." [Online]. Available: https://www.massport.com/environment/environmental-reporting/noise-abatement/how-logan-operates/. [Accessed: 14-May-2017].

[17] Massport, "Massport - Noise Complaints." [Online]. Available: https://www.massport.com/environment/environmental-reporting/noise-

abatement/noise-complaints/. [Accessed: 25-May-2017].
[18] Federal Aviation Administration, “BOS Airport Diagram,” 2017. [Online]. Available: http://aeronav.faa.gov/d-tpp/1705/00058ad.pdf#nameddest=(BOS). [Accessed: 10-May-2017].
[19] Federal Aviation Administration, “FAA Operations & Performance Data.” [Online]. Available: https://aspm.faa.gov/. [Accessed: 15-May-2017].
[20] Google, “Getting Started | Google Maps Geocoding API | Google Developers.” [Online]. Available: https://developers.google.com/maps/documentation/geocoding/start. [Accessed: 14-May-2017].
[21] L. L. Jensen, J. Thomas, C. Brooks, M. Brenner, and R. J. Hansman, “Development of Rapid Fleet-Wide Environmental Assessment Capability,” *AIAA Aviat. Forum*, pp. 1–14, 2017.
[22] L. AirNav, “AirNav: KBOS - General Edward Lawrence Logan International Airport.” [Online]. Available: https://www.airnav.com/airport/KBOS. [Accessed: 10-May-2017].
[23] J. L. Thomas and R. J. Hansman, “MODELING PERFORMANCE AND NOISE OF ADVANCED OPERATIONAL PROCEDURES FOR CURRENT AND FUTURE AIRCRAFT,” 2017.
[24] P. Boone, “NADP 1 (Noise Abatement Departure Procedure 1) NADP 1 NOISE ABATEMENT PROCEDURES NADP 2 (Noise Abatement Departure Procedure 2),” 2006. [Online]. Available: http://www.b737mrg.net/downloads/b737mrg_noise.pdf. [Accessed: 11-May-2017].
[25] Federal Aviation Administration, “Aviation Environmental Design Tool (AEDT) Version 2c.” [Online]. Available: https://aedt.faa.gov/2c_information.aspx. [Accessed: 14-May-2017].
[26] Matlab, “Area of polygon - MATLAB polyarea.” [Online]. Available: https://www.mathworks.com/help/matlab/ref/polyarea.html. [Accessed: 14-May-2017].
[27] Matlab, “Points located inside or on edge of polygonal region - MATLAB inpolygon.” [Online]. Available: https://www.mathworks.com/help/matlab/ref/inpolygon.html. [Accessed: 14-May-2017].
[28] C. Brooks, “Modeling the Effects of Aircraft Flight Track Variability on Community Noise Exposure,” 2017.